# Present-Day Antarctic Climatology of the NCAR Community Climate Model Version 1*

REN-YOW TZENG@ AND DAVID H. BROMWICH@,†

*The Ohio State University, Columbus, Ohio*

THOMAS R. PARISH

*Department of Atmospheric Science, University of Wyoming, Laramie, Wyoming*

(Manuscript received 2 December 1991, in final form 28 April 1992)

ABSTRACT

Five-year seasonal cycle output produced by the NCAR Community Climate Model Version 1 (CCM1) with R15 resolution is used to evaluate the ability of the model to simulate the present-day climate of Antarctica. The model results are compared with observed horizontal syntheses and point data.

Katabatic winds, surface temperatures over the continent, the circumpolar trough, the vertical motion field, the split jet stream over the Pacific Ocean, and the snowfall accumulation are analyzed. The results show that the CCM1 with R15 resolution can well simulate to some extent the dynamics of Antarctic climate not only for the synoptic scale, but also for some mesoscale features (mesoscale cyclogenesis). This is reflected in the zonal-mean pattern of vertical motion by the presence of two convergence centers. The finding suggests that the CCM1 might also capture the split jet stream over New Zealand in winter, but the evidence is mixed. This is inferred to be due to inadequate simulation of the thermal forcing over high southern latitudes. The CCM1 can also capture the phase and amplitude of the annual and semiannual variation of temperature, sea level pressure, and zonally averaged zonal (E–W) wind. That the CCM1 can simulate some characteristics of the semiannual variation may be due to the improved radiation treatment compared to the earlier CCM0.

The most dramatic shortcomings were associated with the model's anomalously large precipitation amounts at high latitudes, which result from the scheme to suppress negative moisture values. The simulations of cloudiness and the atmospheric heat balance are adversely affected. A greatly refined moisture budget scheme is needed to eliminate these problems and may allow the split jet-stream feature over the New Zealand area in winter to be accurately reproduced. A coupled mesoscale–CCM1 model may be needed to adequately simulate the feedback from mesoscale cyclones to synoptic-scale weather systems, and the katabatic wind circulation.

## 1. Introduction

Antarctica is one of the largest energy sinks on earth. The extensive surface radiative cooling of the Antarctic continent is the counterpart to the tropical energy sources. The north–south temperature gradient controls the meridional atmospheric eddy fluxes that transport heat and moisture poleward. Furthermore, the strong surface radiative cooling over Antarctica favors snowfall accumulation, which results in a giant ice sheet over the Antarctic continent. The ice cover over the continent provides long records of climate (e.g., Lorius et al. 1985), but its surrounding sea-ice cover is very dynamic. The oceans not only transport heat poleward, but also transport cold water substance equatorward, such as the equatorward drift of sea ice and icebergs, and the thermohaline circulation in the deep ocean. These features suggest that the high southern latitudes assume a significant role in influencing global climate variability and change (e.g., Stouffer et al. 1989).

Numerical study of global climate is based upon the assumption that the numerical model used is properly formulated both dynamically and mathematically. This is not always the case, however, especially for the subgrid-scale physical parameterizations, the surface-boundary conditions (air–land and air–ocean interactions), and the hydrologic cycles. For instance, Xu et al. (1990) indicated that most general circulation models (GCM) do not adequately simulate many climatic characteristics of high southern latitudes, such as the circumpolar trough (in both location and intensity), the intensity of the stationary eddies, the split jet stream over New Zealand in winter, and the semiannual wave. Boville (1991) pointed out that at high horizontal resolution (T63, triangular truncation at wavenumber 63) the CCM1 can reasonably simulate the winds, eddy fluxes, and eddy kinetic energies in the

* Contribution 799 of Byrd Polar Research Center.

@ Byrd Polar Research Center.

† Atmospheric Sciences Program.

*Corresponding author address:* Dr. David H. Bromwich, The Ohio State University, Byrd Polar Research Center, 108 Scott Hall, 1090 Carmack Rd., Columbus, OH 43210-1002.

Southern Hemisphere, but that serious discrepancies are found at lower resolution. Furthermore, Tucker (1991) indicated that different land–surface exchange parameterizations and the interaction between oceans and atmosphere are also important for model simulations, especially in the Southern Hemisphere.

By contrast, Oglesby (1989) used the NCAR CCM1 to investigate the cause(s) for Antarctic glaciation and pointed out that the oceanic heat transport appears to have a minor role in the formation/elimination of Antarctic glaciation, but that lowering the elevation of Antarctica has a larger effect on the model simulations, reducing the likelihood of glaciated conditions. Elliot et al. (1991) noted, however, that geologic data indicate that polar location and elevation cannot be primary controls on the formation and subsequent fluctuations of the ice sheet [for a slightly different viewpoint see Prentice and Denton (1988)]. Hence, they suggested that an improved geologic database would substantially improve the ability to validate model results. This should be accompanied by improvements in the performance of the models, so that present-day conditions can be simulated with some confidence (cf. Simmonds 1990).

After ice core data from the Antarctic plateau revealed the correlation between surface temperature and carbon dioxide concentration extending back to 160 000 years ago (Jouzel et al. 1987; Barnola et al. 1987), much more attention has been paid to Antarctic climate records by climate-change modelers and paleoclimatologists. Less effort has been made to improve both modeling and observational analysis of this environment, however. In this paper, we intend to use the limited observational database to verify the performance of the NCAR CCM1 in simulating Antarctic climate. Here we concentrate solely on the little-considered Antarctic aspects of the topic even though changes in simulation of the external forcings can have a significant impact (Meehl and Albrecht 1988). Therefore, the main purposes of this paper are to provide a comprehensive explanation of the model deficiencies and to suggest feasible approaches for addressing some of these problems.

## 2. Model description

The model used in this study is the NCAR Community Climate Model Version 1 (CCM1) with R15 (rhomboidal truncation at wavenumber 15) horizontal resolution. The parameterizations of convection, surface processes, vertical diffusion, and radiative transfer are described in Williamson et al. (1987). The R15 horizontal resolution is equivalent to a grid mesh of 4.5° latitude by 7.5° longitude, or about 500-km horizontal resolution. The vertical direction is described by the topographically dependent $\sigma$ coordinate ($\sigma = p/p_s$); there are 12 discrete levels with the lower 7 levels being in the troposphere and the other 5 levels being above the tropopause. The lowest $\sigma$ level is at $\sigma = 0.991$, which is about 65 m over the Antarctic continent and averages 85 m over the sea surface.

Antarctic model topography is adapted from actual topographic data with truncation at R15. The effect of this truncation on model topography is depicted by a north–south vertical cross section of model and real topography along 90°E longitude (Fig. 1). It is clear that the steepest slope of the Antarctic continent is along the coastline instead of over the Antarctic plateau as shown by the model. Furthermore, although the model grid points at 64°S are treated as open ocean or sea ice, the ocean is in fact about 500 m above mean sea level along the model's coastline, with ditches about 100 m deep at 55°S. The effect of the distorted topographic and sea level representation of the model will be discussed further in the next section.

Surface temperatures are calculated over land, snow, and sea ice via a surface-energy budget equation, while the sea surface temperatures (SST) over the open ocean are input from climatological data. The SST are specified and updated in the middle of each month for seasonal cycle simulations. The thickness of sea ice is prescribed to be 2 m. The snow depth and cover change with time in the seasonal cycle run. The seasonal cycle is basically determined by the seasonal change of the SST and the daily change of the solar declination angle with a fixed solar insolation (1370 W $m^{-2}$) at the top of the model. No diurnal cycle is included in the model. The diurnal cycle is expected to be included in the next generation of the CCM1, the CCM2 (Williamson 1990), which is not available at this time.

A standard seasonal cycle simulation has been conducted with the option of interactive surface hydrology, which is similar to Manabe (1969). The soil moisture, snow cover, and in some cases sea ice are computed as functions of time and can thus interact with the other model components. The depth of snow and sea

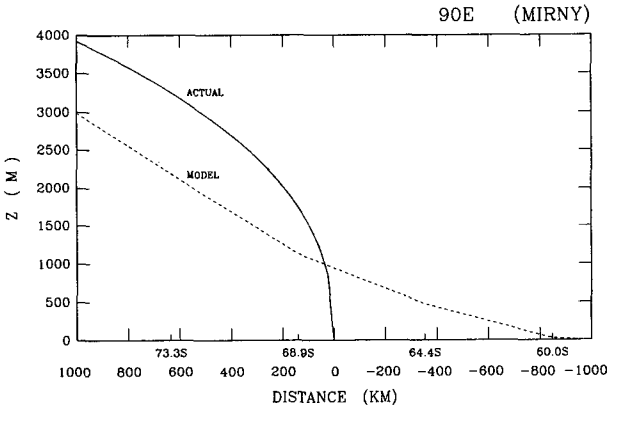


FIG. 1. Antarctic topography along 90°E. Solid line is a fit to the actual terrain inland from Mirny (Parish 1984). Dashed line is the model's terrain representation. Note that the grid points at 64.4°S are treated as ocean.

ice is calculated from the balance between snowfall accumulation, ablation (melting), and evaporation. The snow is assumed to hold no liquid water; that is, all the snowmelt goes into soil moisture. When the soil moisture reaches the maximum water-holding capacity of the soil, the excess part of the liquid water is assumed to form runoff and to flow directly into rivers and oceans.

Precipitation and clouds are computed as the moisture condensed due to the mutual adjustment of temperature and moisture fields (Manabe et al. 1965). Negative moisture values, which can occur because of the spectral representation, are suppressed; this is accomplished by two steps: the local and global moisture fixers. First, the model eliminates the negative specific humidity locally by transporting moisture vertically and longitudinally from adjacent points. If the moisture from these points is not enough to correct a negative value, a globally conserving correction is made after the local correction is applied at all points. In the second step, moisture is added to the points with negative values until nonnegative (zero). To offset the increase in moisture by the process, all values are decreased proportionally. This positive moisture scheme significantly affects the cloud and precipitation calculations in the polar regions (Rasch and Williamson 1990). The effect of this moisture scheme on the model climate is one of the major topics of this paper.

The model forms clouds that interact with the radiation parameterization (Ramanathan et al. 1983). Convective clouds are formed when one or more layers undergo moist convective adjustment. The model assumes that the clouds in each layer are randomly overlapped with a maximum cloud cover of 30% in the convective column and have a cloud emissivity of 1. Nonconvective clouds are formed whenever stable condensation occurs. The fractional cloud cover of these nonconvective clouds is assumed to be 95%, and their emissivity is a function of liquid water content. No clouds of any type are formed in the very thin surface layer of the model nor in the top two layers of the standard 12-level version.

The simulation was performed on the CRAY Y-MP of the Ohio Supercomputer Center (OSC). The model was integrated for six model years, and only the last five years' output was analyzed and saved on cartridge tapes due to the storage limitations at OSC. Two 1200-day perpetual runs (July and January) were also simulated. The results of these two simulations are not shown here because they are very similar to the winter and summer means of the seasonal cycle, respectively, and because these two seasons are not the best times to represent the Antarctic climate, which is strongly influenced by the semiannual variation (van Loon 1967; Schwerdtfeger 1984). Our model output and the NCAR CCM1 history tapes (e.g., Williamson and Williamson 1987) were compared and found to be in agreement.

Two model outputs per day (0000 and 1200 model time) are generated. The monthly averaged values were used for this seasonal cycle study. The model climate was compared to the observed Antarctic climate published in various locations. We also compared the model output to individual weather station data over Antarctica (e.g., Schwerdtfeger 1970, 1984), since the climatological statistics are somewhat uncertain due to the sparse database (Simmonds 1990).

## 3. Results

### *a. Surface winds*

The Antarctic katabatic wind regime is a thermally direct circulation with strong surface radiative cooling as its driving force. This circulation is usually described as a mesoscale phenomenon, especially when its vertical scale is considered, but actually has a continent-wide horizontal dimension. The observed depth of the katabatic wind is usually less than 300 m (Streten 1963; Tauber 1960). The lowest vertical level of the CCM1 over the Antarctic plateau is about 65 m and about 85 m over the ocean, however. Furthermore, there are only two vertical levels within 1000 m from the model surface. It is important to know how well the CCM1 with such coarse vertical and horizontal resolution can simulate the Antarctic katabatic winds.

The winter (July) mean of the simulated surface winds at $\sigma = 0.991$ superimposed on the model topography is displayed in Fig. 2a. As mentioned previously, it is difficult to directly compare the horizontal depictions of model results with those of the observations because the observational data are often sparse and somewhat uncertain. Parish and Bromwich (1991, hereafter referred as PB91) have shown that their mesoscale model is able to produce a realistic katabatic wind regime (Fig. 2b) over the Antarctic continent during the winter season. Therefore, the surface winds from the CCM1 will be compared with those from PB91's mesoscale model. The significant vertical shear between the surface (2 m) and the first CCM1 $\sigma$ level ($\sim$65 m) is not taken into account by this comparison, however. As a result, the first $\sigma$-level wind field is oriented in more of a contour-parallel direction. PB91 indicate that their katabatic regime is directed in a more downslope sense, representing the flows near the surface. Despite these differences, the surface winds of the CCM1 show a similar flow pattern to that of PB91. As expected, the major difference from PB91's result is that the CCM1 does not capture the fine structure of katabatic winds along the west coasts of the Ross and Weddell seas and over the Amery Ice Shelf. This problem is mainly caused by the model resolution, and hence the model is only able to capture the broadscale characteristics of the katabatic winds. The other difference is that the maximum katabatic wind speed simulated by the CCM1 ($\sim$10 m s$^{-1}$) is located over

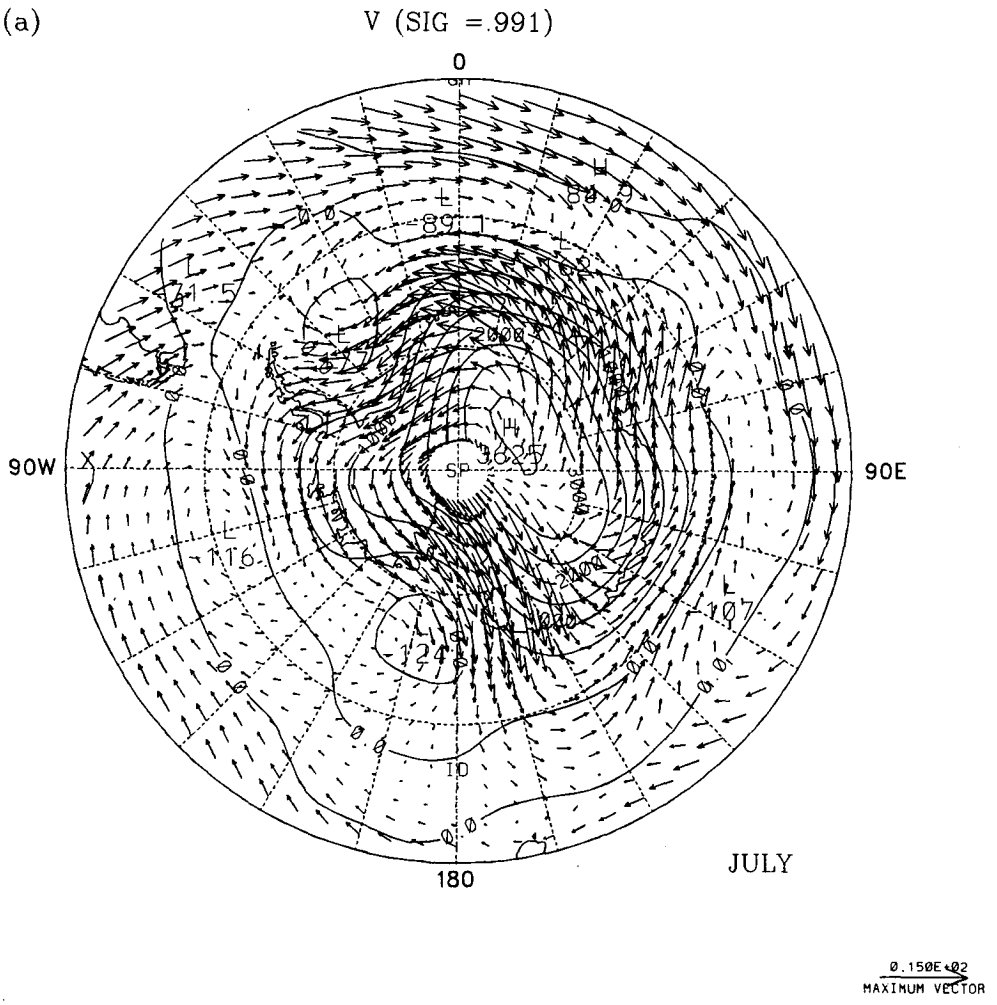


FIG. 2a. The winter (July) mean of the CCM1 simulated surface ($\sigma$ = 0.991) winds. The northern edge of the geographic background is at the 45°S parallel. The contour lines are the model terrain with 500-m contour interval.

the inland part of the continent (the steepest slopes) instead of over the coastal areas as shown by the observations ($\sim$10 m s$^{-1}$). This problem is clearly due to the anomalous model slope, as shown in Fig. 1, that follows from the coarse horizontal resolution.

Figure 3 shows the monthly averaged surface wind speed and direction for three Antarctic weather stations and the corresponding CCM1 output. These stations are Vostok (on the East Antarctic plateau), Byrd (in West Antarctica), and Mawson (a katabatic wind station on the coast of East Antarctica). The monthly averaged model wind speed and direction at Vostok are consistent with the observations. At Mawson, the simulated wind direction is consistent with the observations, while the simulated wind speed is about 2 to 5 m s$^{-1}$ weaker than observed. The model also seems to exaggerate the annual cycle of wind speed over the East Antarctic coast. The weaker wind speed in the model may result from the terrain slope; as mentioned earlier, the slope is much smaller in the model than the real topography, especially near the coast. Moreover, PB91 have shown that the maximum katabatic winds tend to occur over the steepest slope areas. On the other hand, the weakened wind speed during the southern summer might be related to the smaller temperature contrast between the continent and ocean. The smaller land–sea temperature contrast is a result of the overestimated Antarctic surface temperature and will be discussed in the next section. The third station, at Byrd, is located near the saddle point of the West Antarctic continent. The model does not capture this terrain well, so the simulated wind direction is totally out of phase with the observations. The wind speed is also smaller than observed. This is consistent with the terrain shape in that the model slope is smoother than the real terrain near Byrd.

Furthermore, the zonally averaged model zonal wind ($u$) at $\sigma$ = 0.991 shows a significant semiannual vari-

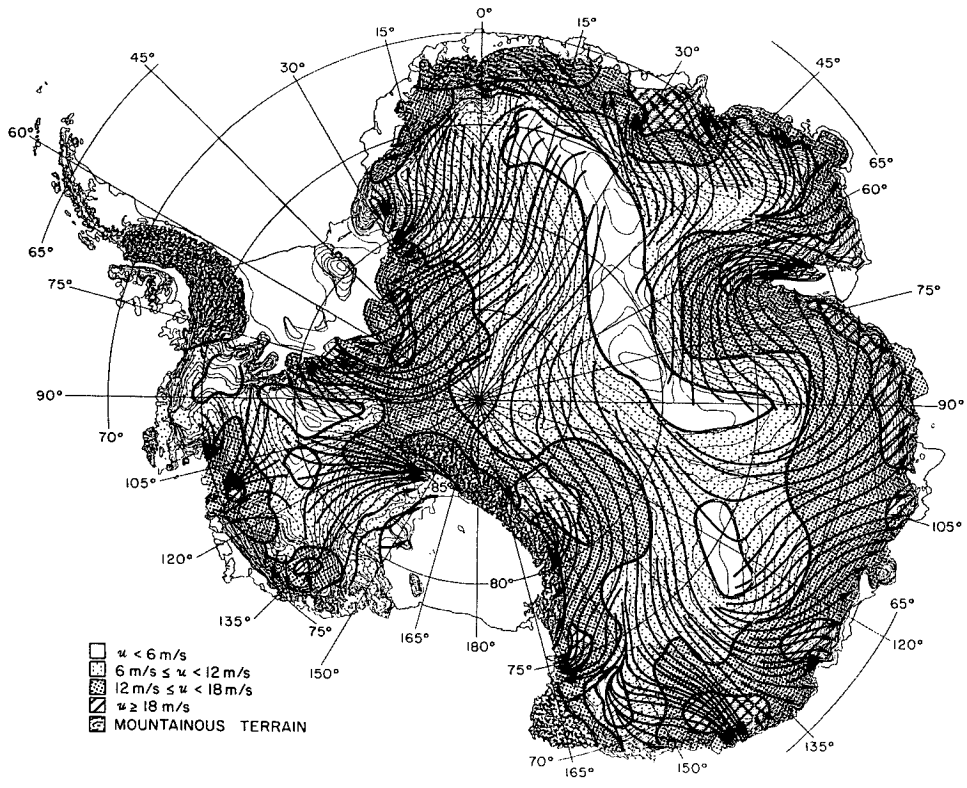


FIG. 2b. The streamlines and speeds of katabatic winds simulated by the mesoscale model of Parish and Bromwich (1991), from Giovinetto et al. (1992).

ation over the Southern Ocean between 50° and 65°S (Fig. 4), although the wind speed is about one-half of the observed. The semiannual cycle reaches a maximum in April and October and a minimum in June and December, which is mostly consistent with the observations (Schwerdtfeger 1984); by contrast, Xu et al. (1990) indicated that the NCAR CCM0 failed to simulate the semiannual cycle of the zonal-mean winds. Therefore, the CCM1 shows a significant improvement in simulating the surface wind over high southern latitudes.

### *b. Surface temperature and inversion strength*

Extremely low surface temperatures and the strong surface inversion are two other important aspects of Antarctic climate in the winter season. The strong surface radiative cooling in winter plays a major role in the formation and maintenance of the katabatic wind circulation (Schwerdtfeger 1984). Furthermore, the Antarctic surface temperature is one of the important variables that monitor the change of glacial and global climate, but, as stressed by many studies (e.g., Xu et al. 1990), many models' Antarctic surface temperatures are about 10°–15°C warmer than the observations (Taljaard et al. 1969; Schwerdtfeger 1970), especially over the Antarctic plateau. Unfortunately, the CCM1 faces the same problem. Moreover, there is no explanation in the literature as to why the CCM1 overestimates the Antarctic surface temperatures.

This problem could be due to the lower altitude of Antarctic topography in a lower-resolution (R15 or T21) spectral model, that is, the spectral truncation problem. Figure 5 shows the observed, model-simulated, and topographically adjusted model surface temperatures at Mawson and Vostok stations. After a topographic adjustment [to the same altitude as the real topography using a representative lapse rate along the snow surface of 1°C/100 m (Radok 1973)], the simulated surface temperature along the coastline (Mawson, Fig. 5a) is much closer to the observations, though the annual fluctuation of the model is a little too strong and the semiannual variation of the model seems too weak. This means that the model cannot capture the coreless (nearly constant) temperature in the winter around the coastline (van Loon et al. 1972). Schwerdtfeger (1984, Fig. 5c) has shown that the coreless seasonal temperature fluctuation is almost entirely composed of annual and semiannual components. Interestingly, this type of temperature fluctuation is well simulated by the model over the Antarctic continent (Fig. 5b). Therefore, the model to some extent can

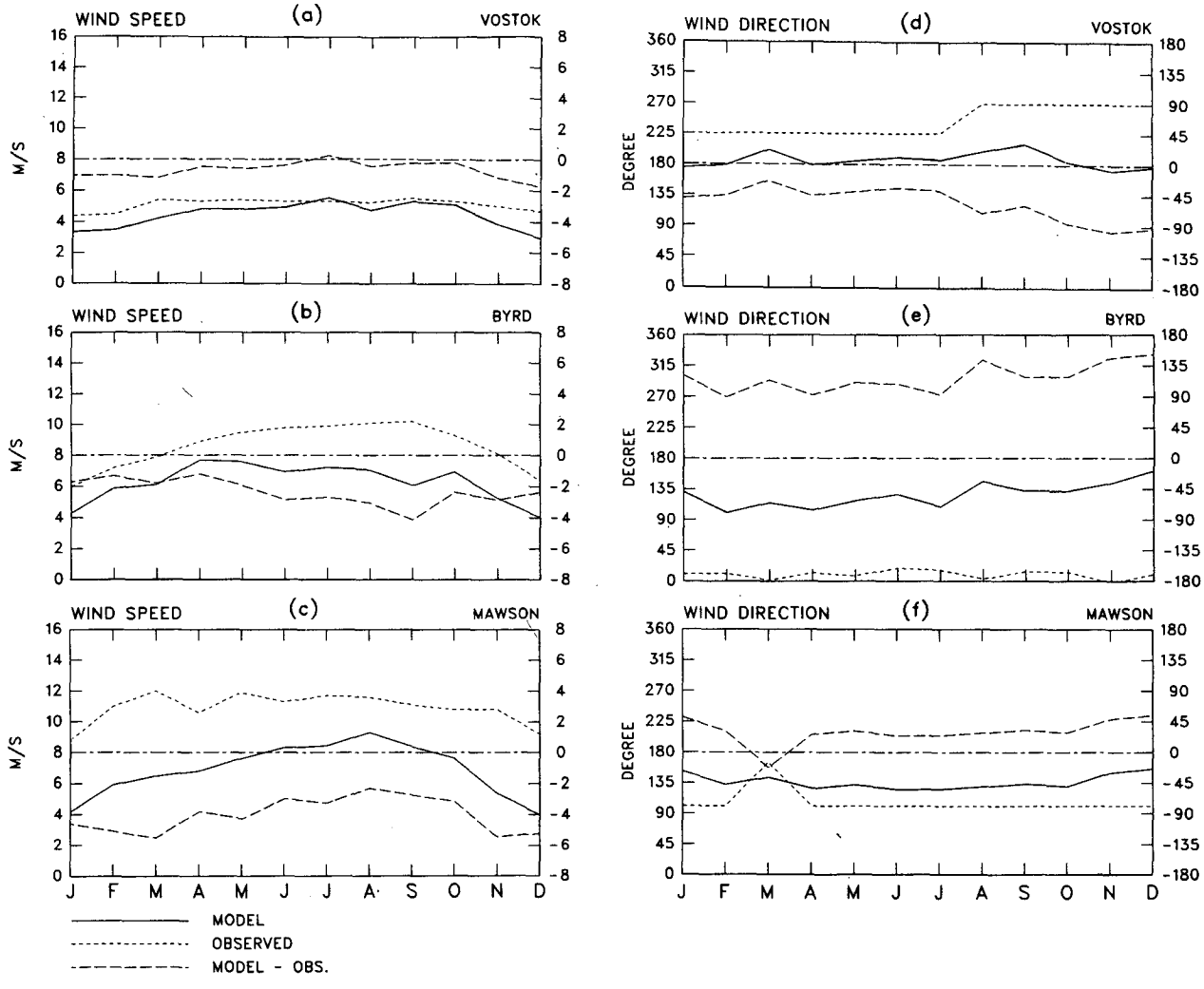


FIG. 3. The seasonal cycle of the model and observed surface wind speeds and directions (scales at left) at Vostok, (a) and (d); Byrd, (b) and (e); and Mawson, (c) and (f). The difference scale is given on the right-hand side.

well simulate the annual and semiannual cycle of temperature fluctuations over the Antarctic plateau, even though the absolute temperature values are too high.

By contrast, the topographic adjustment for Vostok is very small (Fig. 5b), because the elevation of Vostok in the model is almost the same as its actual value. Therefore, the simulated high temperature over the plateau ($\sim$15°C too warm at Vostok) is not due to the elevation difference. In addition, the inversion strength (the temperature difference between the highest temperature in troposphere and the surface) over the Antarctic continent (Fig. 6) is approximately the same as that shown by the observations. This indicates that the temperatures above the surface inversion are also overestimated by the model (compare Randel and Williamson 1990). It is clear that there must be some other mechanism causing the anomalous simulated temperatures over the Antarctic plateau.

Moreover, we also find that the model cloudiness over the Antarctic continent is greatly overestimated. The sky over the Antarctic continent is simulated to be almost overcast for the entire winter (Oglesby 1989). This result is opposite to the observations, in which the sky has less than four-tenths of cloud cover over the Antarctic continent (Schwerdtfeger 1970; van Loon et al. 1972; Yamanouchi and Kawaguchi 1992). The cloud will directly affect the radiative exchange processes (Shibata and Chiba 1990), especially the surface longwave radiation. Therefore, the greenhouse effect (and secondarily the latent heat release from cloud formation over the Antarctic continent) should be the major mechanism to increase the temperature in the troposphere. Further discussion of the overcast situation is contained in the section on snowfall accumulation.

### c. *Sea level pressure (SLP)*

Many studies (e.g., those of Schlesinger 1984; Xu et al. 1990) have pointed out that almost every GCM

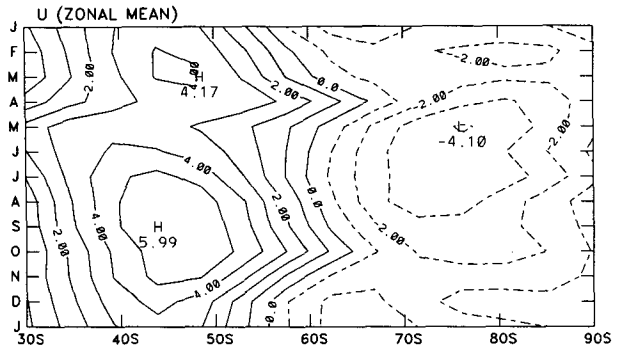


FIG. 4. Latitude–time depiction of zonally and monthly averaged model zonal wind ($u$) component at $\sigma = 0.991$. The contour interval is 1.0 m s$^{-1}$.

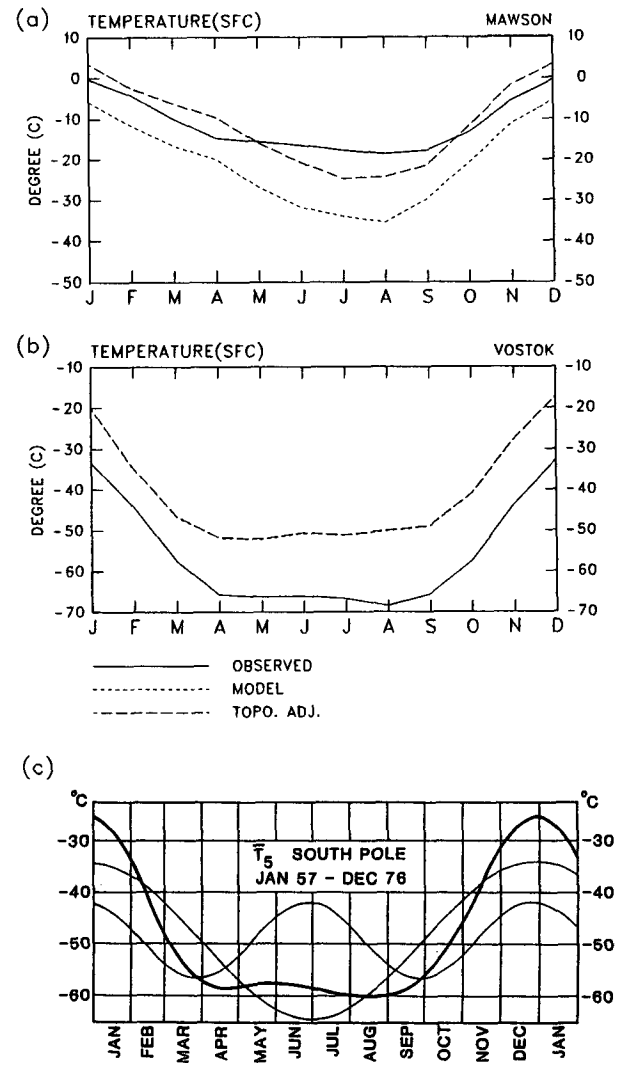


FIG. 5. The seasonal cycle of monthly mean surface air temperature (°C) at (a) Mawson and (b) Vostok. The long-dashed line is the model simulation after topographic adjustment. (c) The seasonal cycle of observed temperature at the South Pole (heavy line) with annual and semiannual waves superimposed (adapted from Schwerdtfeger 1984).

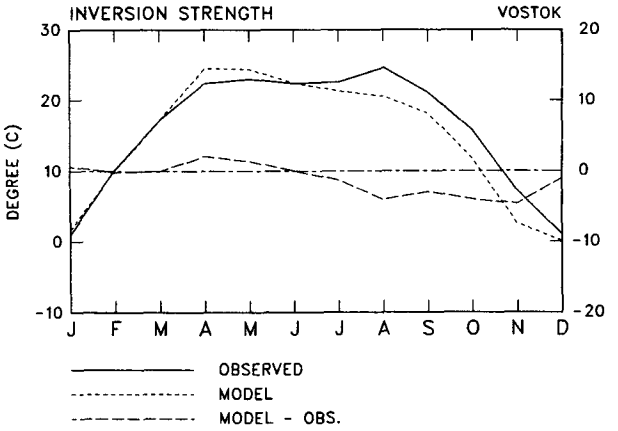


FIG. 6. The seasonal variation of surface inversion strength (°C) at Vostok.

cannot correctly simulate the circumpolar trough both in terms of location (too far north) and intensity (too weak). The CCM1 also has this problem, although a higher-resolution (e.g., T42 or T63) version of the CCM1 may improve the simulated SLP (Hart et al. 1990; Boville 1991). Hart et al. found, however, that the impact is less in the winter season (July).

Figure 7 shows the summer (DJF) and winter (JJA) mean of SLP. It is interesting that the longitudinal locations of the depression centers (at 30°E, 160°E, 140°W, 110°W, and 30°W in the summer, Fig. 7a; and at 10°E, 90°E, 140°W, and 70°W, in the winter, Fig. 7b) are broadly consistent with those of the observations (Figs. 7c and 7d) in spite of their locations being 6° latitude too far north. The latitudinal locations of the model circumpolar trough are in accord with the model "ditches" (Fig. 2a). Therefore, this northward shift of the circumpolar trough is primarily due to the model topographic representation, that is, the horizontal resolution problem (Boville 1991). Another significant difference from the observations is that the observed depression center over the Ross Sea is not well simulated by the model. This may be due to the model resolution and its katabatic wind circulation. We have shown that the katabatic winds over the west coast of the Ross Sea and Ross Ice Shelf are poorly simulated by the model. There are no eastward-directed katabatic flows in this area, and hence the low over the Ross Sea is too weak and too far east in the model. Furthermore, the central pressures of the model trough are about 15 hPa too high in both summer and winter.

Xu et al. (1990) also stressed that most of the GCMs failed to simulate the semiannual variation over the Southern Hemisphere, except over the Pacific sector in the CCM0 (Meehl 1991). Comparing the SLP of CCM1 with that of CCM0 and other GCMs (Figs. 8a and 8b), we found that the CCM1 exhibits a significant improvement in simulating the zonally averaged semiannual variation of SLP including the poleward shift and deepening of the circumpolar trough around the

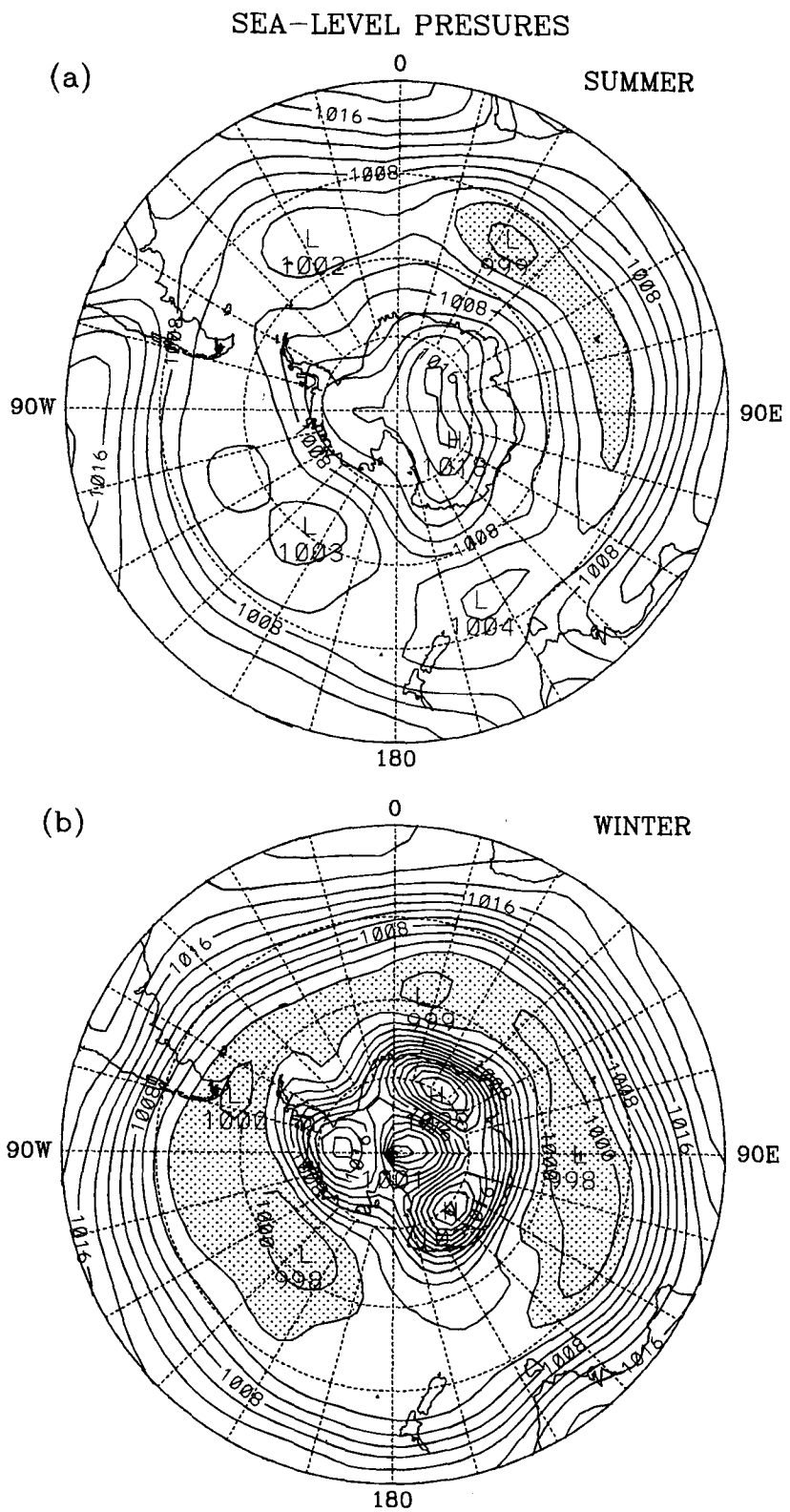


FIG. 7. The summer (DJF) and winter (JJA) mean of the model and observed sea level pressure. (a) and (b) are from the model simulations. (c) and (d) are from observations. The contour interval is 2.0 hPa in (a) and (b), and 4.0 hPa in (c) and (d). Values less than 1002 hPa are

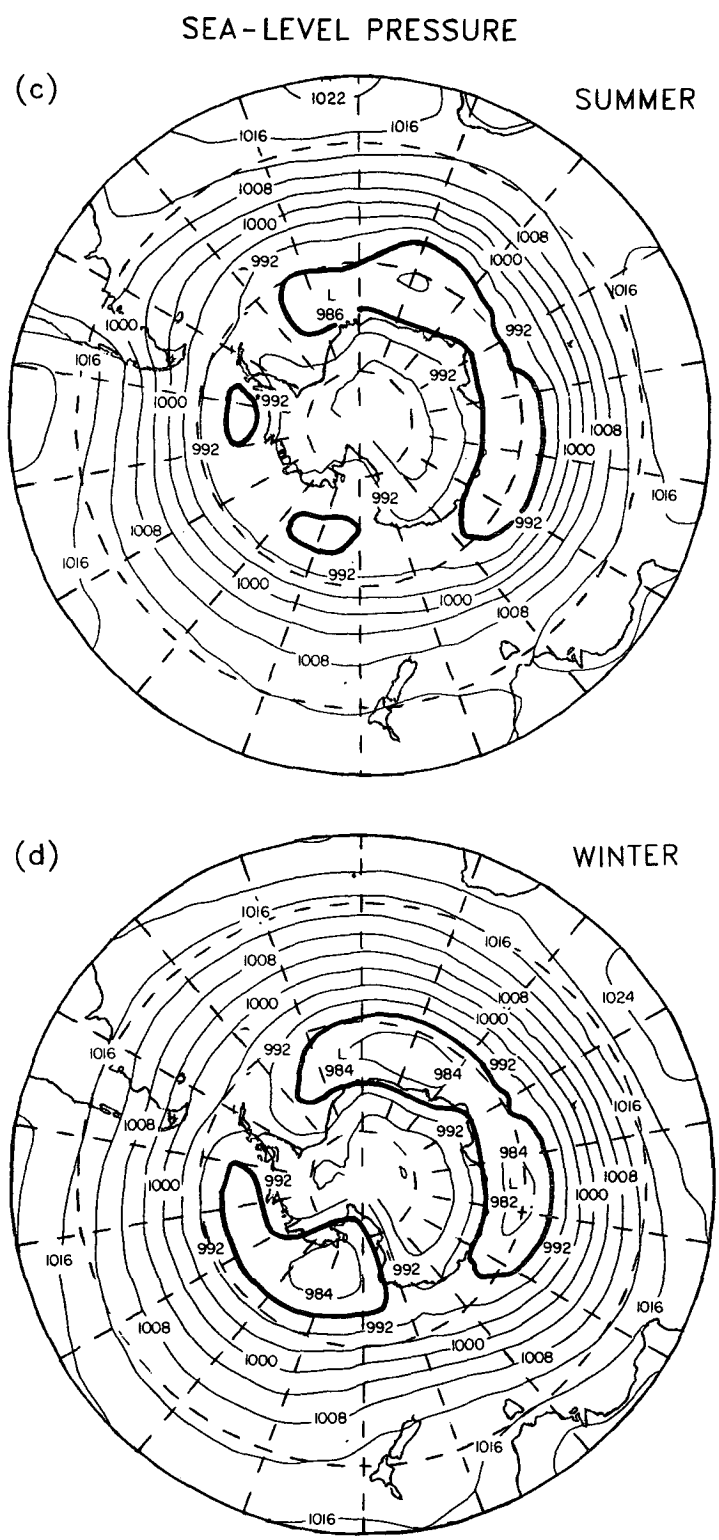


FIG. 7. (*Continued*) shaded in (a) and (b). The bold lines in (c) and (d) are the 988-hPa isobars. (c) and (d) are modified from Simmonds (1990). The northern edge of the polar stereographic plots in this and subsequent figures (except Fig. 16b) is at 30°S parallel.

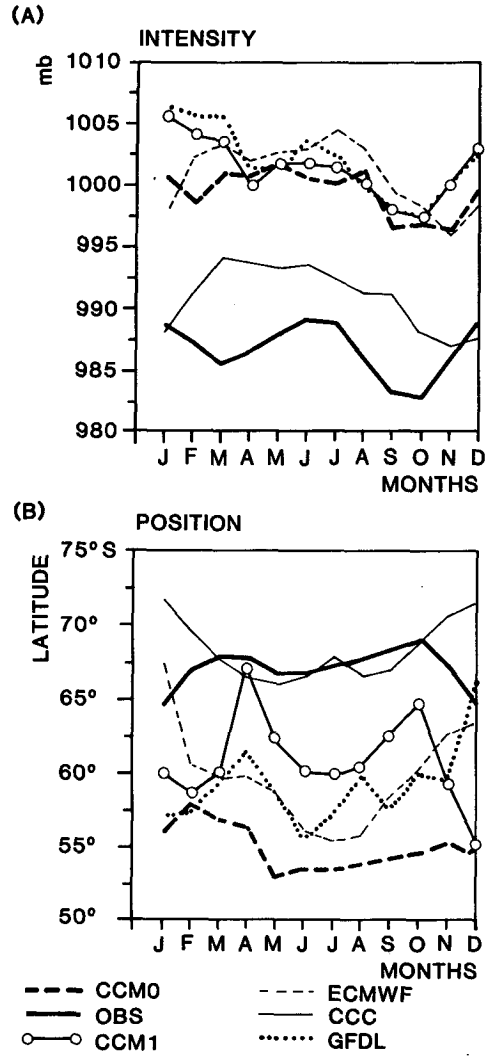


FIG. 8. The annual march of the zonally averaged (a) intensity (hPa) and (b) location (°S) of the circumpolar trough in the observations, CCC model, the NCAR CCM0 and CCM1, the GFDL model, and the ECMWF model. (After Xu et al. 1990 except the CCM1 results.) (CCC: the Canadian Climate Center; GFDL: Geophysical Fluid Dynamics Laboratory; ECMWF: European Centre for Medium-Range Weather Forecasts.)

time of the equinoxes. Interestingly, the phase of the modeled semiannual wave and the intensity variation closely approximate the observations. During the spring and autumn seasons, the centers of circumpolar trough can reach to the south of 65°S (Fig. 8b), which almost coincides with the observed location; however, the summer and winter trough locations are more than 5° latitude too far north.

### *d. Vertical motion ($\omega$)*

Besides SLP, the vertical motion ($\omega$) is the other quantity to effectively show the intensity of depressions. The vertical motion can better represent the activity of mesoscale processes, since this field has high spatial variability. Because the observational data over high southern latitudes are sparse, it is impossible to obtain a complete picture of vertical motion from the observations. Therefore, the simulated vertical motion is used to study the characteristics of the model circumpolar trough and model katabatic wind circulations.

Figure 9a shows the time series of the zonally and monthly averaged vertical motion ($\omega$). It clearly shows that two upward motion (negative) centers exist in late autumn (April and May), one at 45°S and the other at 65°S. These two upward motion (convergence) centers correspond to the polar front and to the Antarctic katabatic wind circulation, respectively. When the season changes from fall to winter, the katabatic wind reintensifies the high-latitude convergence center and the midlatitude convergence center migrates poleward. These two convergence centers become joined in late winter (August); then the katabatic wind circulation rapidly decays in spring and early summer. At the same time, the polar front intensifies and continues to move poleward, merging with the high-latitude center by March.

The horizontal depiction of the July (winter) mean vertical motion (Fig. 9b) clearly shows the two upward motion bands (~45°S and ~65°S), especially over the Indian and Pacific Ocean sectors. Moreover, a significant upward motion center is located over the Ross Sea. This center is consistent with the mesoscale cyclogenesis center over the southwestern Ross Sea found by Bromwich (1989, 1991). Downward motion is simulated over the active mesoscale cyclogenesis area in the Weddell Sea, however (e.g., Turner and Row 1989).

The convergence center over Antarctic coastal areas suggests that the model is able to capture the activity of mesocyclones over this region, as shown by automatic weather station observations and satellite imagery (Bromwich 1989; Heinemann 1990; Fitch and Carleton 1992; Bromwich 1991). Confirmation is provided by Murray and Simmonds (1991) who found a secondary maximum in cyclogenesis at high southern latitudes in the Australian spectral GCM (R21). Furthermore, although the horizontal resolution of the CCM1 (R15) is relatively coarse (about 500-km grid spacing) in middle latitudes, the E–W resolution is about 280 km at 70°S due to the poleward convergence of the meridians. Therefore, the model may be able to capture the mesoscale cyclonic activity in high latitudes, although it is still unclear how this simulated activity is actually manifested. Also, the interactions between this mesoscale cyclonic activity and the synoptic-scale depressions are not well documented by the observations and model results. Therefore, it is important to further investigate these topics. Finally, the relationship between the vertical motion and other fields (precipitation rate and cloudiness) is also discussed in the section on snowfall accumulation.

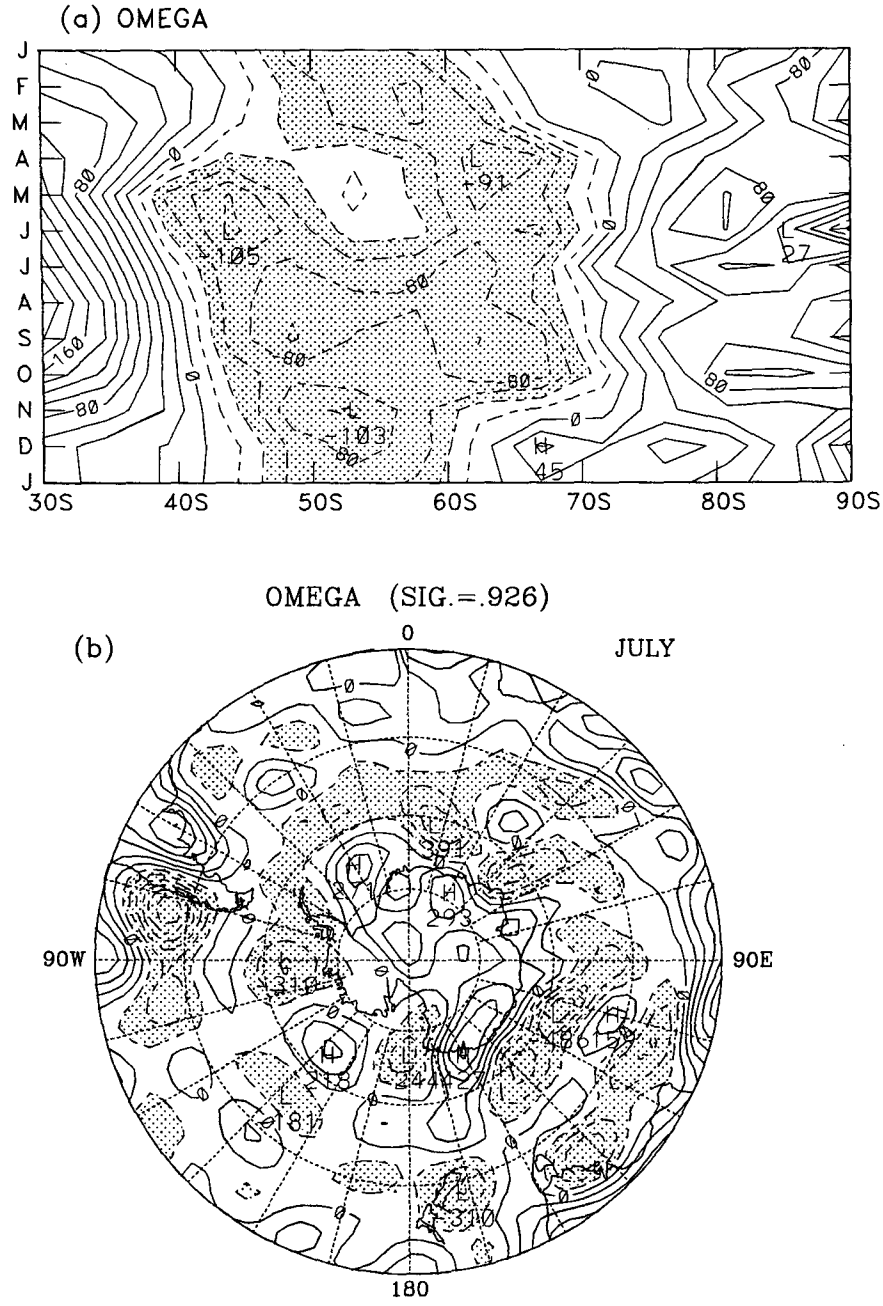


FIG. 9. Latitude–time plot of the model vertical motion ($\omega$) in (a), and in (b) the winter (July) mean of $\omega$ at $\sigma = 0.926$ (near the model surface). The contour interval is 0.002 hPa $s^{-1}$ in (a) and 0.01 hPa $s^{-1}$ in (b). The values less than $-0.004$ hPa $s^{-1}$ are shaded in (a) and less than $-0.01$ hPa $s^{-1}$ in (b); contour values have been multiplied by $10^4$.

*e. Split jet stream*

A recurring question is why the CCM1 cannot simulate the split jet stream feature over the New Zealand area in winter. By analyzing the meridional temperature gradient, we found that two maximum temperature gradient bands (35° and 70°S) show up at low levels in the Pacific sector during winter (Fig. 10). This implies that two baroclinic zones exist in these areas. Moreover, from thermal wind considerations we know that a strong baroclinic zone is accompanied by a jet stream. Therefore, we may expect that another jet stream may exist in high southern latitudes over the Pacific sector. The horizontal wind, however, does not

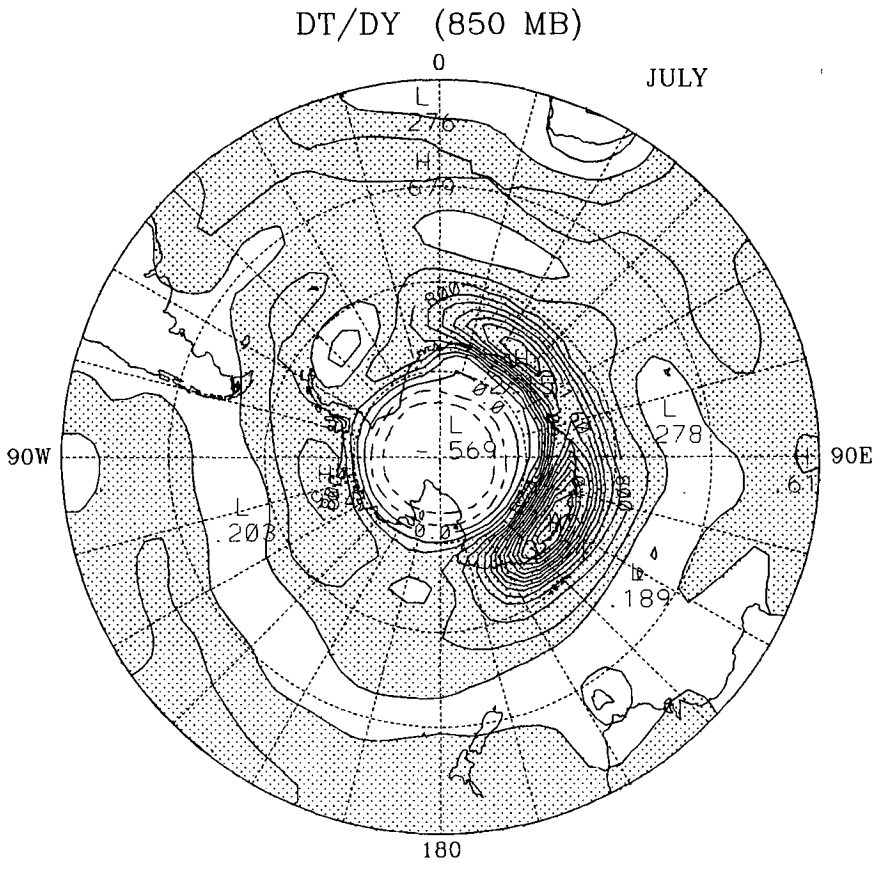


FIG. 10. July mean of meridional temperature gradient at 850 hPa. Contour interval is 0.2°C per degree latitude, and values greater than 0.2 are shaded. For clarity, the analysis poleward of 82°S has been suppressed, and the dashed lines there have no physical meaning.

clearly exhibit this signal (e.g., Xu et al. 1990) even in a high-resolution version of the CCM1 (T63; Boville 1991).

By analyzing the vertical cross section of zonal (E–W) wind averaged over the Pacific sector, Kitoh et al. (1990) found that their model can simulate a double-jet pattern (subtropical and polar jets) similar to the observations over this sector. Interestingly, the vertical cross section of the CCM1 simulated zonal wind (Fig. 11a) also shows a similar double-jet feature (Fig. 11c) in this sector (one at 40°S from surface to tropopause, the other at 65°S from 700 hPa to 300 hPa). Moreover, the locations of the modeled double jet are consistent with the simulated maximum meridional temperature gradient (Fig. 11b). The only differences between the CCM1's simulated jet streams and the observations are their locations and the intensity. The CCM1's polar jet stream is somewhat too weak and about 5° latitude too far poleward. The reason for these deficiencies in the model would be the same as those for the katabatic wind circulation and the thermal forcing, because this jet stream is also part of this thermally direct circulation. In other words, the absence of the split jet stream in the horizontal wind pattern is due not only to the model resolution, but also to the temperature distribution; that is, because the simulated surface temperatures over the continent are too warm the land–sea temperature contrast for this area is too small.

### *f. 500-hPa geopotential height*

Figure 12 exhibits the simulated and observed January and July mean of 500-hPa geopotential height. The simulated circumpolar vortex intensifies from January to July as in the observations. However, as shown with the circumpolar trough, the simulated low center is about 150–300 gpm higher than that observed in both January and July. In section 3b, we pointed out that the overestimated cloudiness affects the temperature simulation underneath the cloud cover, which extends from the surface to 250 hPa (Fig. 13b). Therefore, the anomalously high 500-hPa heights are due to the model's tropospheric warm bias (which increases the lower tropospheric thickness) and to the elevated surface pressures.

Moreover, the location of the wavenumber-one low center and the planetary-scale wave pattern are also misplaced by the model. The observed low centers are

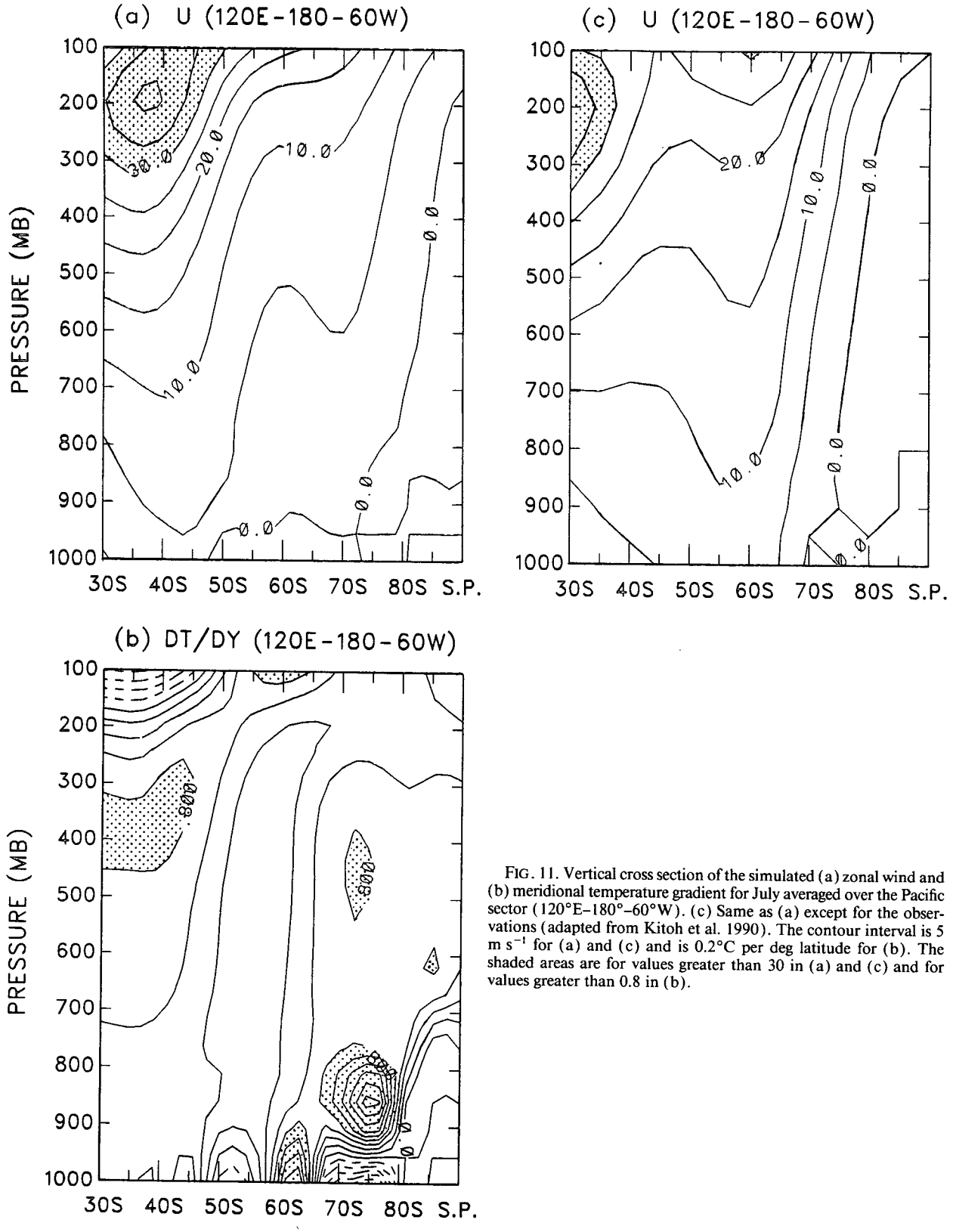


FIG. 11. Vertical cross section of the simulated (a) zonal wind and (b) meridional temperature gradient for July averaged over the Pacific sector (120°E–180°–60°W). (c) Same as (a) except for the observations (adapted from Kitoh et al. 1990). The contour interval is 5 m $s^{-1}$ for (a) and (c) and is 0.2°C per deg latitude for (b). The shaded areas are for values greater than 30 in (a) and (c) and for values greater than 0.8 in (b).

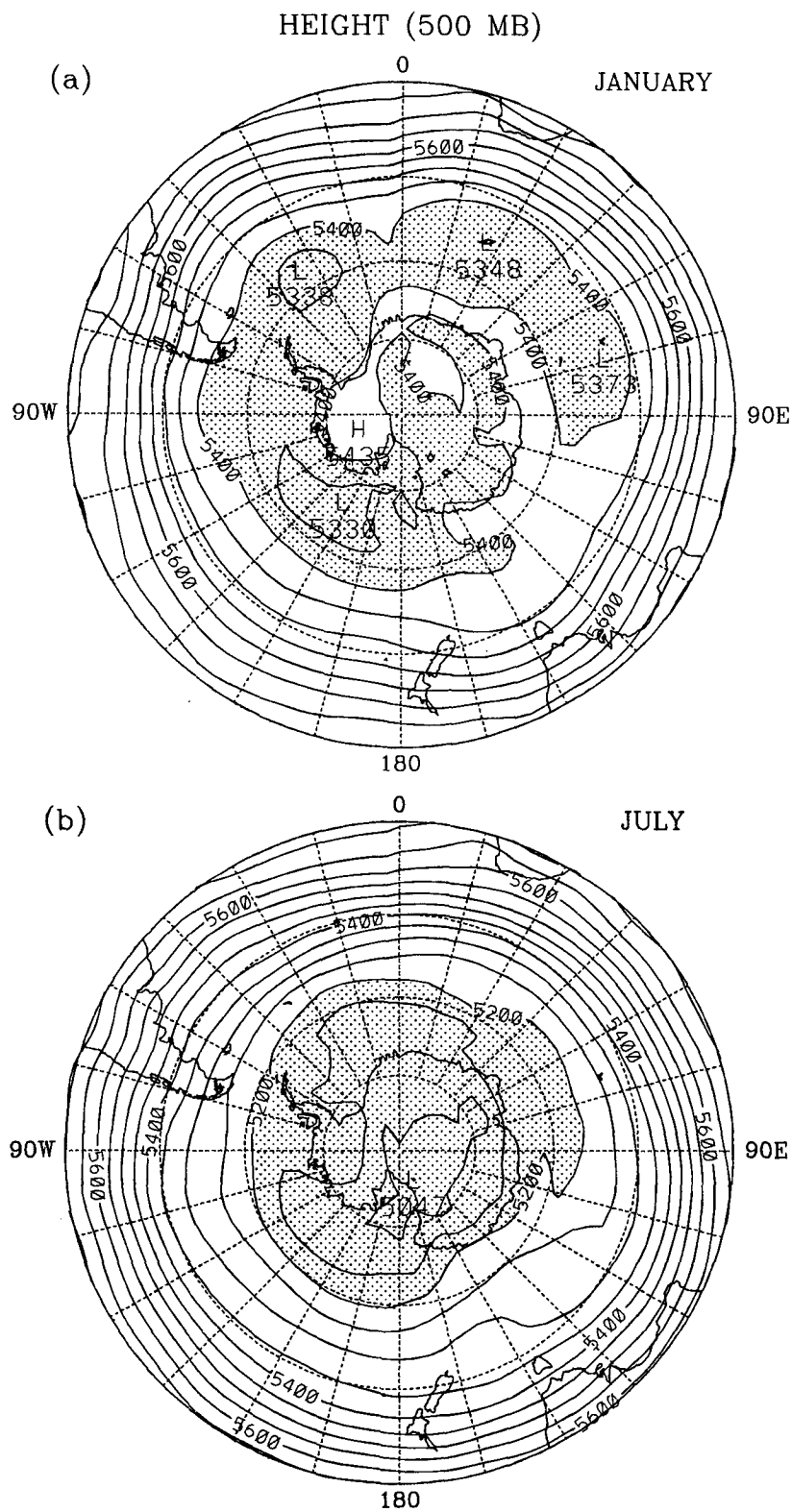


FIG. 12. The January and July mean of 500-hPa geopotential height field for the model, (a) and (b), and from the observations, (c) and (d) (adapted from van Loon et al. 1972). The contour interval is 50 gpm in (a) and (b), but 8 dam in (c) and (d). Values less than 5400 gpm

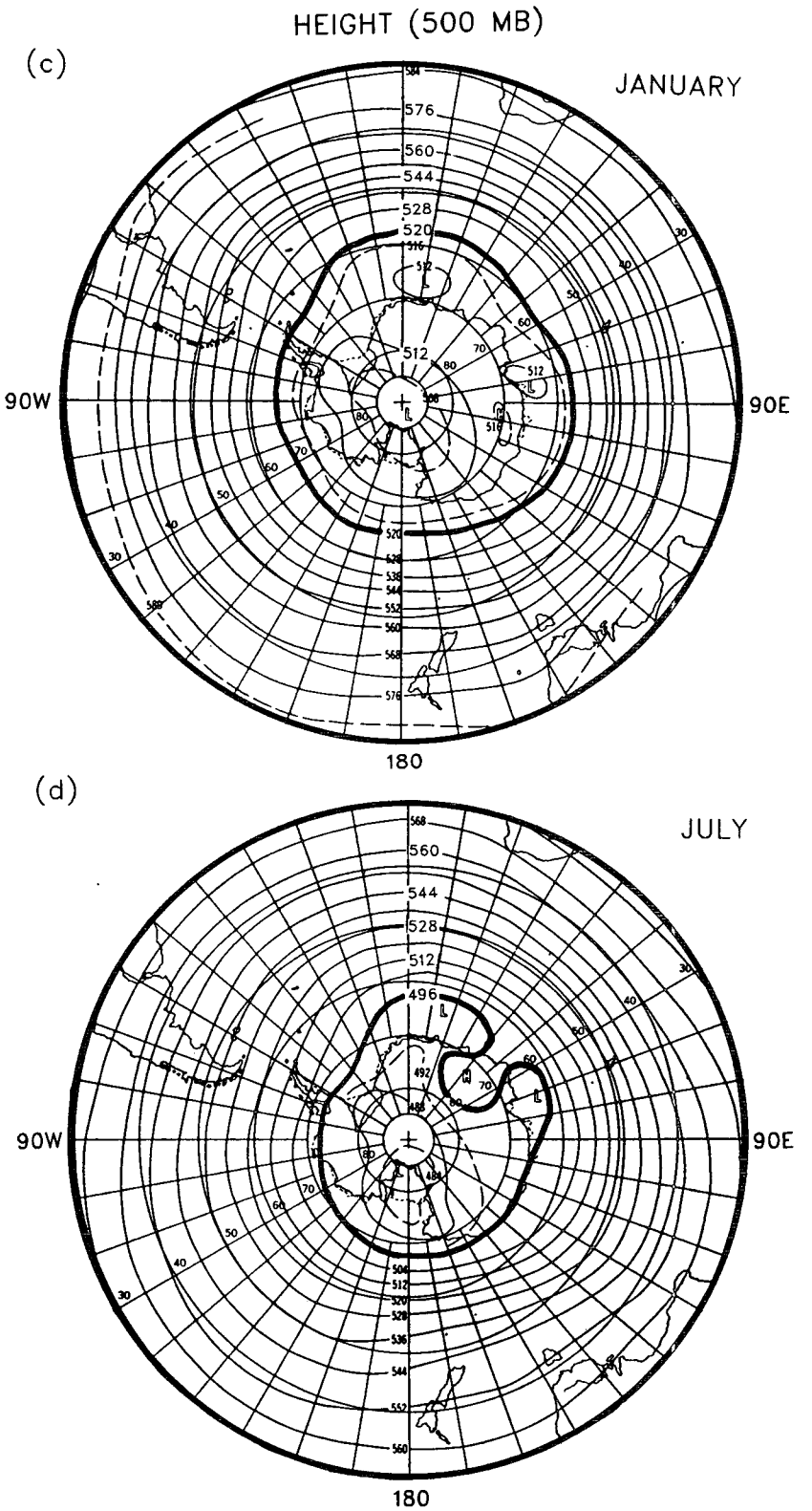


FIG. 12. (*Continued*) are shaded in (a) and less than 5200 gpm in (b). The 520- and 496-dam isohypses are bolded in (c) and (d), respectively.

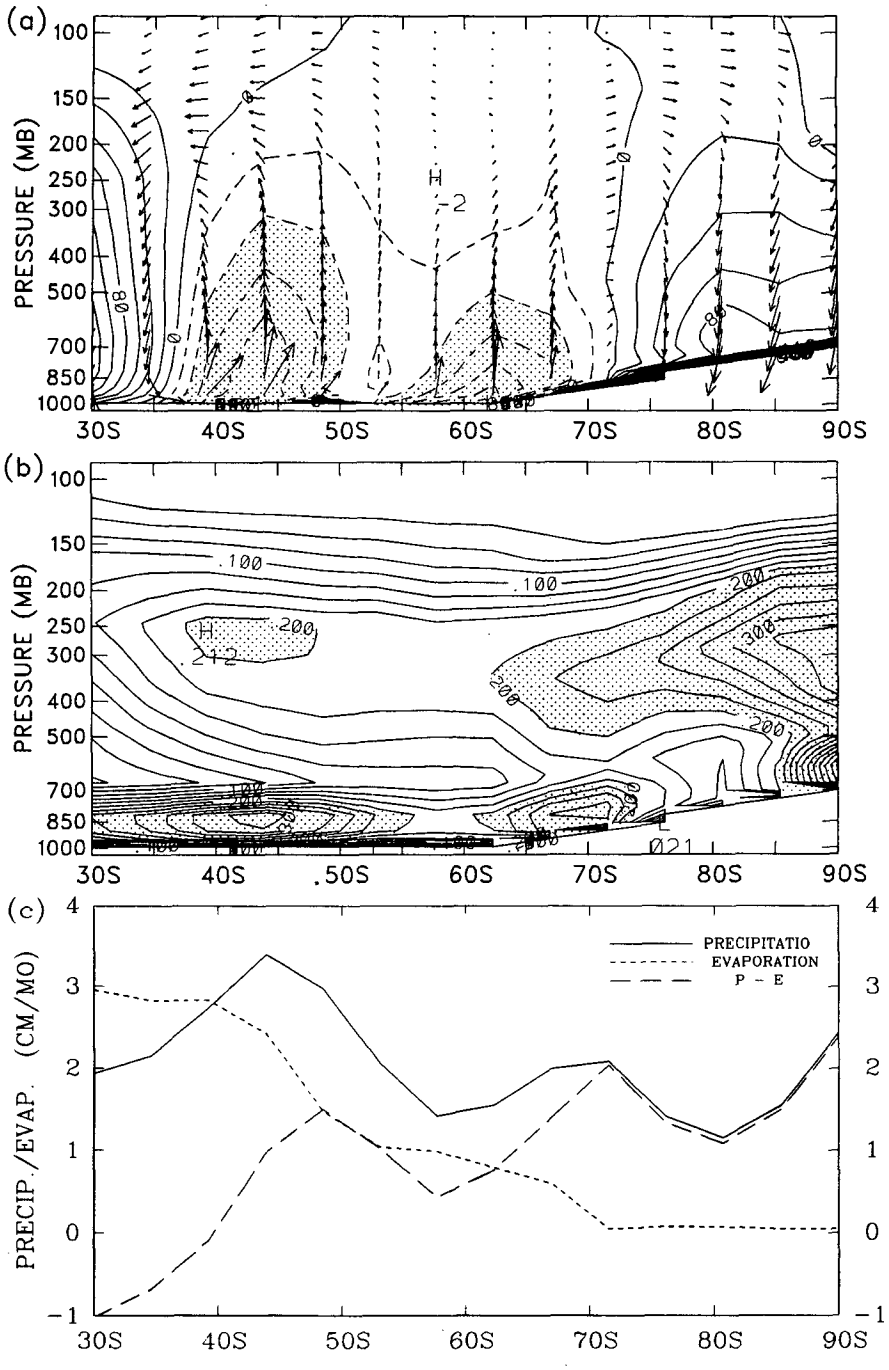


FIG. 13. The vertical cross section of the model zonally averaged meridional–vertical wind ($v$-$\omega$) vectors superimposed with the zonal mean of $\omega$ in (a); in (b), the vertical cross section of zonal mean cloudiness; and in (c), the zonal mean of precipitation ($P$), evaporation ($E$), and the net precipitation ($P$–$E$). The contour intervals are 0.002 hPa $s^{-1}$ ($\times 10^4$) in (a) and 0.025 in (b). Values less than $-0.004$ hPa $s^{-1}$ are shaded in (a), and values greater than 0.2 are shaded in (b).

at 150°E in January and at 170°W in July (Figs. 12c and 12d), but they are almost over East Antarctica in the model. Because the planetary-scale waves are maintained by the topographic and the thermal forcing, this problem can be attributed to either that the model does not correctly represent the Antarctic topography or that the model miscalculates the heating source (sink) over the Antarctic continent. Using a spectral

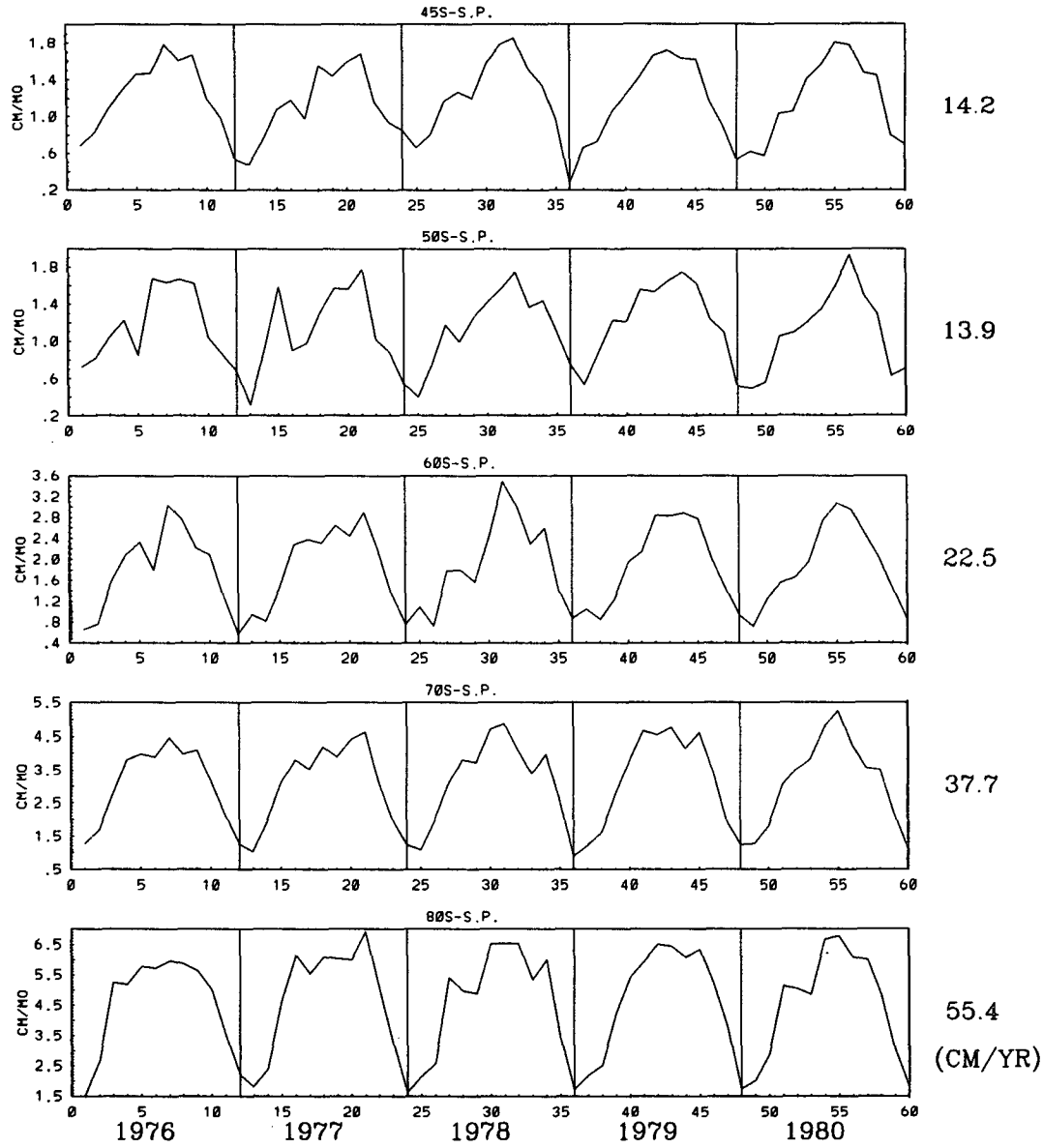


FIG. 14. The annual cycle of the residual term of the moisture budget equation [right-hand side minus left-hand side of Eq. (2)]. The number on the right edge of each panel is the annual average for that area.

model with T42 resolution to study the forcing of planetary-scale Rossby waves by Antarctica, however, James (1988, 1989) was able to recreate a correct wavenumber-one pattern and mimic the split jet stream over the New Zealand region. Moreover, Boville (1991) showed that the high horizontal resolution (T63) version of CCM1 does not capture the split jet-stream pattern over this region either, despite the greatly improved topographic representation. Therefore, the misplacement of this wavenumber-one low center by the CCM1 is more likely due to the thermal forcing. This argument is consistent with the finding on surface winds, surface temperature, and the split jet stream that the temperature distribution over the Antarctic continent is substantially misrepresented by the model.

### *g. Snowfall accumulation*

The accumulation of snowfall on the Antarctic continent is one of the major factors determining the response of the ice sheet to climatic change. The annual precipitation rate of the CCM1 is substantially larger than observed, however (Elliot et al. 1991), although the simulated seasonal cycle is qualitatively representative and the horizontal distribution in a very large scale sense is well simulated (Simmonds 1990). A de-

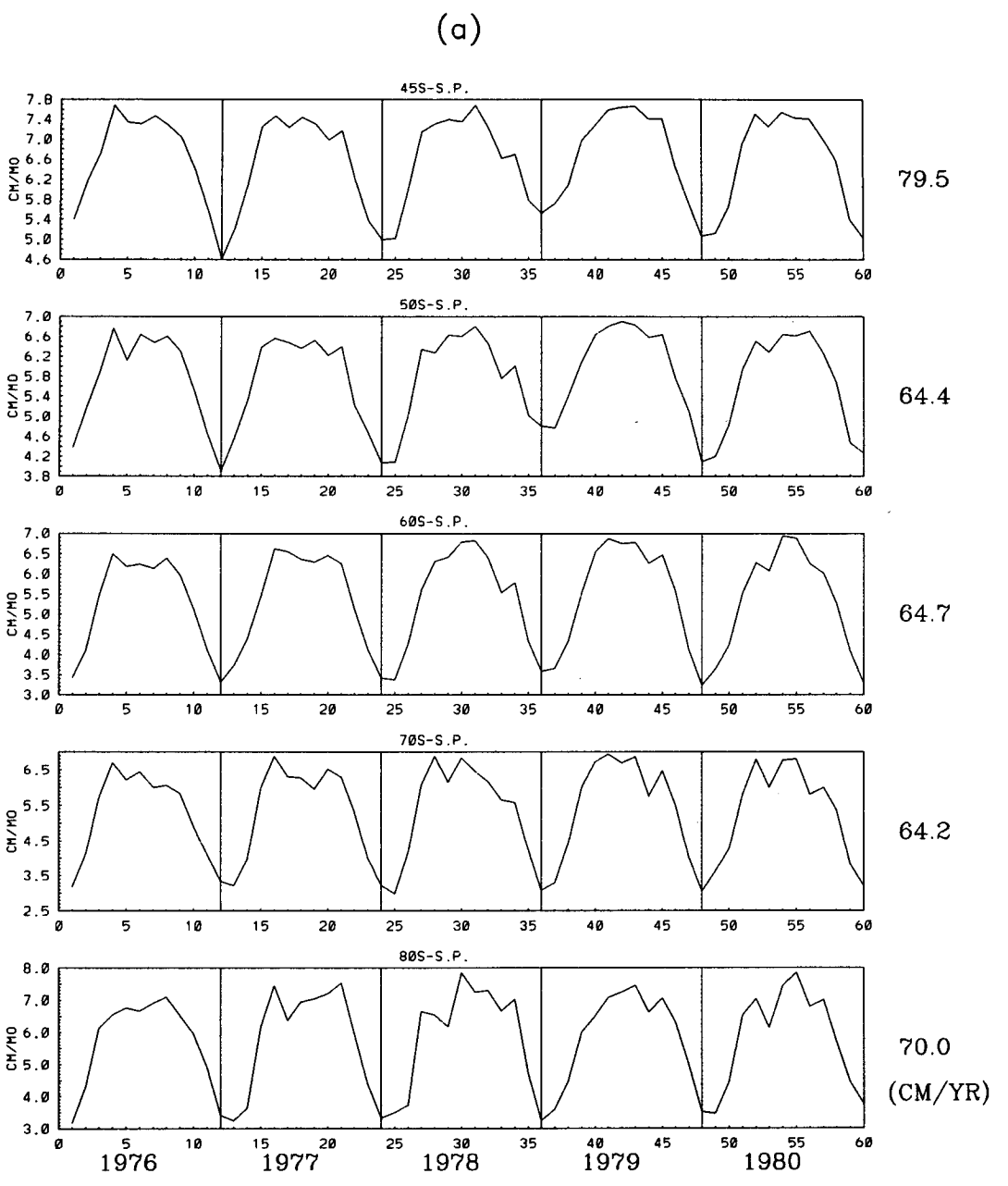


FIG. 15. Areally averaged precipitation rate for the model (a). The annual average is given on the right edge of each panel. Observed precipitation rate at stations (b) along the coast of East Antarctica and (c) in the interior of the continent (from Bromwich 1988). In (b) and (c), the numbers in parentheses after each station are the annual average in centimeters per year.

tailed analysis of the model's snowfall accumulation is discussed below.

The temporally and spatially averaged version of the atmospheric moisture-balance equation (Peixoto and Oort 1983) is

$$\langle \partial \bar{W}/\partial t \rangle + \langle \nabla \cdot \bar{Q} \rangle = \langle \bar{E} - \bar{P} \rangle, \qquad (1)$$

where precipitable water ($W$) is

$$W = \int_0^{P_s} \frac{q}{g}\, dp$$

and the horizontal moisture transport vector ($\mathbf{Q}$) is

$$\mathbf{Q} = \int_0^{P_s} q \frac{\mathbf{V}}{g}\, dp.$$

The angle brackets indicate a spatial average, $q$ represents specific humidity, $g$ the gravitational acceleration, $\mathbf{V}$ the horizontal wind vector, $P$ precipitation, $E$ evaporation, $p$ pressure, and $p_s$ surface pressure. The vapor budget is established for the entire atmospheric volume overlying the area of interest. The zonally averaged

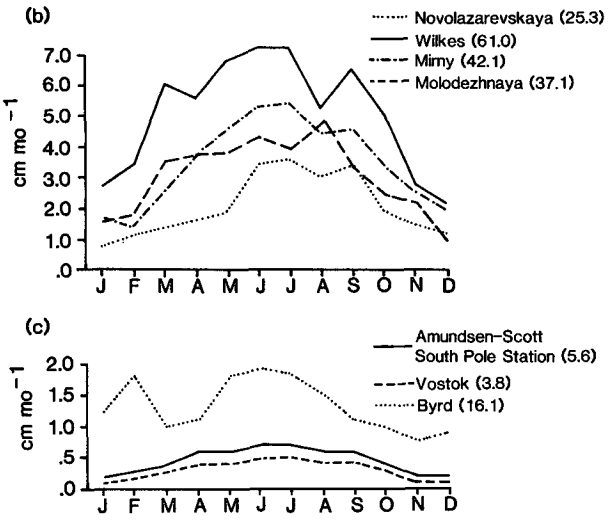


FIG. 15. (*Continued*)

version of Eq. (1) on a monthly time scale can be written as

$$\frac{1}{a\cos\varphi}\frac{\partial[\bar{Q}_\varphi]\cos\varphi}{\partial\varphi} = [\bar{E} - \bar{P}], \qquad (2)$$

where $a$ is the radius of the earth, $\varphi$ is the latitude, $Q_\varphi$ is the moisture transport in the meridional direction, and the square brackets denote a zonal average.

The zonal mean of precipitation rate (and accumulation) is consistent with that of cloudiness and vertical motion; Fig. 13 shows the results for May. Figure 13c shows three precipitation peaks at 45°S, 70°S, and the South Pole (SP). The two precipitation maxima over midlatitude and subpolar regions are consistent with the convergence centers (Fig. 13a) discussed in the section on vertical motion. The third precipitation maximum over the Antarctic continent is totally due to the artificial positive moisture fixer (Rasch and Williamson 1990). This problem can be clearly exhibited by the residual term of the moisture-balance equation [right-hand side minus left-hand side of Eq. (2)]. Figure 14 shows a monotonously increasing error of the moisture budget with respect to latitude. The amplitude of this error is almost the same as the simulated total snowfall accumulation within the 80°S latitude and the error is about 58% within the 70°S parallel. Therefore, it is clear that the CCM1 is not appropriate for climate-change studies that rely on snowfall accumulation; for example, within the 70°S parallel the simulated accumulation rate ($P$–$E$) is 3.5 times larger than observed (Giovinetto et al. 1992). Moreover, the moisture fixer scheme is also responsible for the overcast sky simulated over the continent. This cloudy sky then causes many other serious problems, such as the anomalously warm troposphere, the misplacement of the 500-hPa low center of wavenumber one, and so on, as indicated and supported by Shibata and Chiba (1990).

In addition, analysis of the heat budget was also conducted in this study by applying the same approach used in Eqs. (1) and (2) to the thermodynamic equation. As expected, the heating sources and the transports were grossly out of balance over high southern latitudes because of the anomalous heating source from the artificial positive moisture fixer.

Though the total snowfall accumulation over Antarctica is wrong in the model, the annual cycle of simulated precipitation rate over the continent is consistent with the observations (Fig. 15). Moreover, the horizontal distribution of annual net precipitation rate ($P$–$E$, in Fig. 16b) is similar to the observations (Fig. 16a), with a broad minimum over the East Antarctic plateau, minima over the Ross Ice Shelf and the Filchner/Ronne Ice Shelf, and three coastal accumulation maxima. These three maximum centers are associated with the convergence (surface upward motion) centers along the Antarctic coastline (Fig. 9b). Note the anomalous maximum near the South Pole (see Fig. 13).

On the other hand, R. J. Oglesby (1991, personal communication) suggested that the two minimum accumulation centers over West Antarctica (Fig. 16b) might result from the impact of Antarctic topography. In CCM1 simulations with R15 resolution, however, one cannot prove that this accumulation pattern is really due to some physical process(es), because the truncation error at these latitudes is so large that it can mask any real phenomenon. An easy way to evaluate this truncation error is to specify zero accumulation at all grid points south of 60°S, then convert the gridpoint data to spherical harmonics with R15 resolution and transfer the spectral data back to the gridpoint domain. Surprisingly, one finds that the snowfall accumulation pattern after this conversion is very similar to that of the original model output. Therefore, it is uncertain as to how the CCM1 can simulate these accumulation minima. Higher horizontal resolution could help to resolve the truncation problem, but Rasch and Williamson (1990) indicated that the impact of the positive moisture fixer is relatively insensitive to resolution beyond T42. Therefore, we may need either to redesign the positive moisture scheme or to couple a mesoscale model with the CCM1, for example, Giorgi (1990) and Giorgi et al. (1990), to resolve this problem.

## 4. Conclusions and remarks

In this paper we have used five-year CCM1 seasonal cycle simulation output to investigate the performance of the NCAR CCM1 in simulating Antarctic climate. Many important Antarctic climate features are discussed in this study. They are katabatic winds, surface temperatures, inversion strengths, sea level pressures, vertical motion, split jet streams, geopotential heights, and snowfall accumulation. Some important conclusions are summarized as follows:

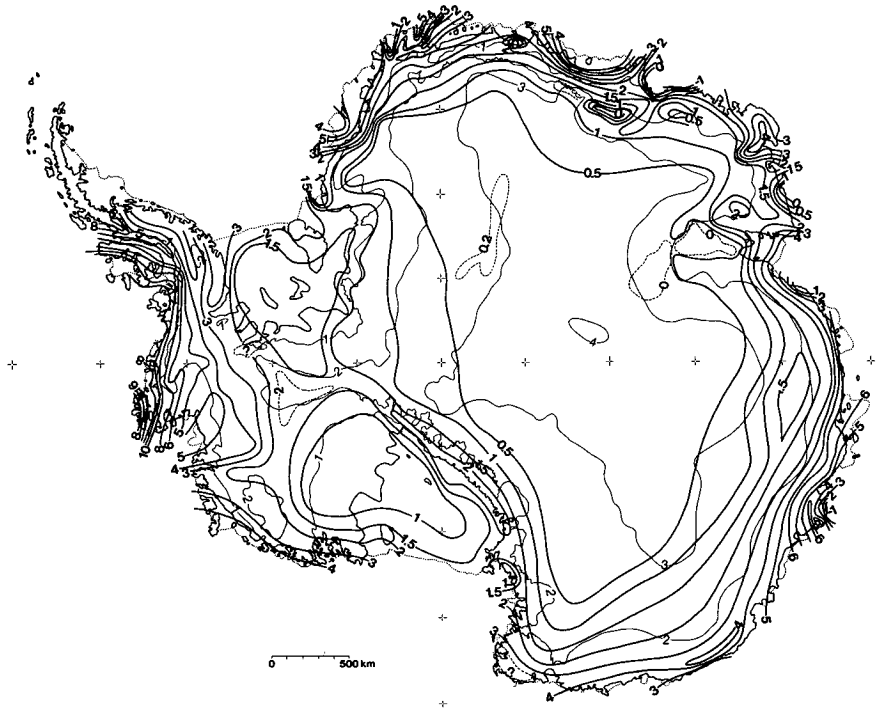


(b) ANNUAL ACCUMULATION

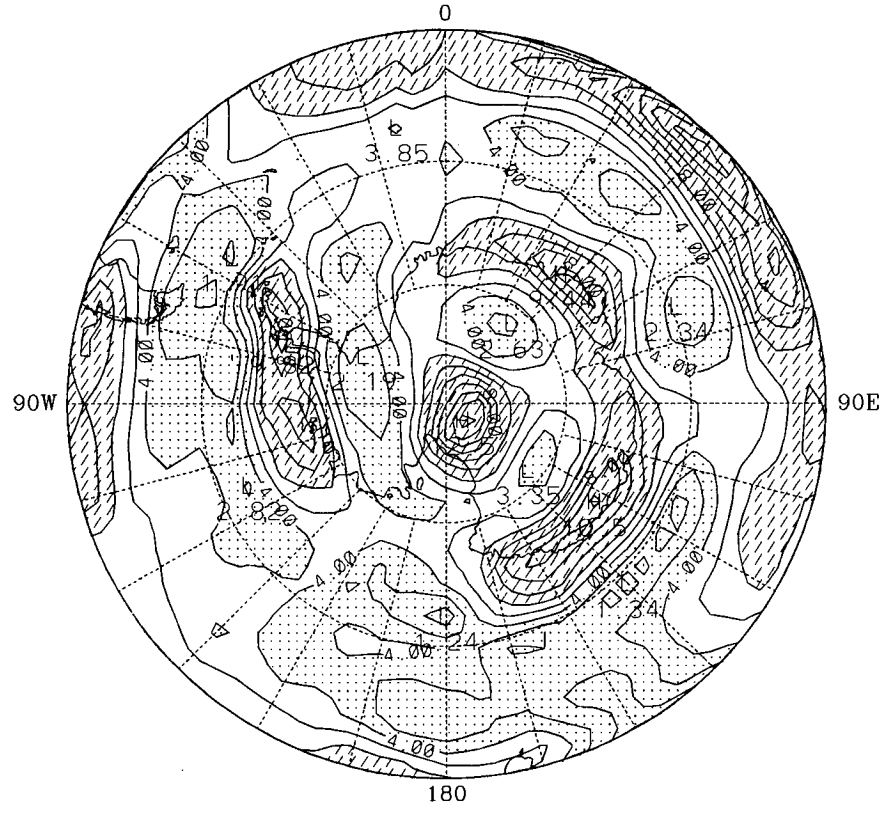


FIG. 16. The annual snowfall accumulation ($P$–$E$) from (a) the observations (adapted from Bromwich 1988, and in turn modified from Giovinetto and Bentley 1985) and (b) the model. Unit: 100 mm yr$^{-1}$. Contour interval in (a) is variable and in (b) is 100 mm yr$^{-1}$. In (a), the thin lines are elevation contours in kilometers. In (b), values less than 400 mm yr$^{-1}$ are stippled and greater than 600 mm yr$^{-1}$ are hatched; northern boundary is at 45°S parallel.

- To some extent, the model can simulate the seasonal cycle well: for example, katabatic winds, surface temperatures, sea level pressures, 500-hPa geopotential heights, and precipitation rate. Their horizontal distributions and amplitudes are broadly consistent with those observed, but all these model fields exhibit large biases. In particular, the circumpolar trough is too far north and not deep enough. This may be due to the model's topography and spectral truncation.
- The phase and amplitude of the semiannual variation of the model's SLP and zonally averaged zonal wind ($u$) are consistent with the observations, but the locations are not properly simulated. Contrasting winter and summer may not be the correct way to study Antarctic climate, because the semiannual variation is such an important phenomenon.
- The model may be able to capture the split jet stream over the New Zealand area in the winter, if the thermal forcing can be properly simulated. This deficiency of the model is also believed to result from the moisture scheme.
- The moisture budget is poorly simulated over the Antarctic continent. There is too much precipitation and cloud over the continent. Hence, the temperature over the continent is also overestimated due to the greenhouse effect. This problem is directly linked to the artificial positive moisture fixer. A better positive moisture scheme (e.g., the semi-Lagrangian transport schemes of Rasch and Williamson 1990) is expected to be implemented in the new version of the CCM (CCM2; Williamson 1990). In its present form, the model is not suitable for climate-change applications that rely on snowfall estimates over Antarctica.
- The subpolar convergence over the coastline may be related to mesoscale cyclogenesis. For a better understanding of this phenomenon, detailed study of the behavior of cyclones in the CCM1 is needed, and is being conducted.

It is encouraging that the NCAR CCM1 can simulate the semiannual variation better than that of the CCM0 and some other GCMs. The reason for this improvement is still unclear. The substantial changes between the CCM0 and the CCM1, however, must be responsible for this; the revised radiation scheme (Williamson et al. 1987) is the likely cause, because the simulated planetary albedo over the Antarctic continent (not shown) also shows a very large semiannual variation. In contrast, Meehl (1991) emphasized the importance of the oceanic heat storage near 50°S.

The horizontal resolution is also an important factor influencing the model results. This is more serious over the polar regions, because the two poles are singular points for spherical harmonics. To adequately address many aspects (e.g., mesoscale cyclogenesis and katabatic winds), it may be necessary to couple a mesoscale model with the CCM1. High horizontal resolution may not be sufficient to remedy all problems, however, because the model is also very sensitive to many parameterizations: for example, the radiative processes, surface–atmosphere interactions, cloud processes, soil hydrology, and moisture budget. Therefore, a sensitivity study of the model to these parameterizations is also important to understand and improve its performance. In contrast, however, the simulated Antarctic climate is influenced by the fraction of open water (leads) in the sea-ice cover surrounding the continent (Simmonds and Budd 1991). This will make the model simulation even worse, since the inclusion of leads in the model will increase the tropospheric temperatures and precipitation over Antarctica.

Finally, it is interesting to point out the contrast between the Antarctic katabatic wind and the Indian monsoon circulation. Basically, these two circulations are the same in a thermally direct sense—one induced by strong surface cooling and the other by massive heating. They occur in the same season with one over the south polar area and the other over the tropics.

*Acknowledgments.* This work was supported in part by an internal grant of The Ohio State University (RYT) and in part by NASA Grants NAGW-2718 to D. H. Bromwich and NAGW-2666 to T. R. Parish. The NCAR CCM1 code used here is the standard version made available by NCAR to institutions belonging to the University Corporation for Atmospheric Research; it was ported to run at the Ohio Supercomputer Center (OSC) by Mr. David F. Knight. The computations were mostly performed on the CRAY Y-MP of OSC, which is supported by the State of Ohio, and the remainder on the CRAY Y-MP of NCAR, which is sponsored by the National Science Foundation. The computational (CPU) time on the NCAR CRAY Y-MP was provided by CRAY Research Inc.

## REFERENCES

Barnola, J. M., D. Raynaud, Y. S. Korotkevich, and C. Lorius, 1987: Vostok ice core provides 160 000 year record of atmospheric $CO_2$. *Nature,* **329,** 408–414.

Boville, B. A., 1991: Sensitivity of simulated climate to model resolution. *J. Climate,* **4,** 469–485.

Bromwich, D. H., 1988: Snowfall in high southern latitudes. *Rev. Geophys.,* **26**(1), 149–168.

——, 1989: Subsynoptic-scale cyclone developments in the Ross Sea sector of the Antarctic. *Polar and Arctic Lows,* P. F. Twitchell, E. A. Rasmussen, and K. L. Davidson, Eds., A. Deepak, 331–345.

——, 1991: Mesoscale cyclogenesis over the southwestern Ross Sea linked to strong katabatic winds. *Mon. Wea. Rev.,* **119,** 1736–1752.

Elliot, D. H., D. H. Bromwich, D. M. Harwood, and P.-N. Webb, 1991: The Antarctic glacial geologic record and GCM modeling: A test. *Proc. Int. Conf. on the Role of the Polar Regions in Global Change,* Fairbanks, 508–516. [Geophys. Inst., University of Alaska, Fairbanks, Fairbanks, AK 99775.]

Fitch, M., and A. M. Carleton, 1992: Antarctic mesocyclone regimes from satellite and conventional data. *Tellus,* **44A,** 180–196.

Giorgi, F., 1990: Simulation of regional climate using a limited area model nested in a general circulation model. *J. Climate,* **3,** 941–963.

——, M. R. Marinucci, and G. Visconti, 1990: Application of a

limited area model nested in a general circulation model to regional climate simulation over Europe. *J. Geophys. Res.*, **95,** 18 413–18 431.

Giovinetto, M. B., and C. R. Bentley, 1985: Surface balance in ice drainage systems of Antarctica. *Antarct. J. U.S.*, **20**(4), 6–13.

——, D. H. Bromwich, and G. Wendler, 1992: Atmospheric net transport of water vapor and latent heat across 70°S. *J. Geophys. Res.*, **97,** 917–930.

Hart, T. L., W. Bourke, B. J. McAvaney, and B. W. Forgan, 1990: Atmospheric general circulation simulations with the BMRC global spectral model: The impact of revised physical parameterizations. *J. Climate*, **3,** 436–459.

Heinemann, G., 1990: Mesoscale vortices in the Weddell Sea region (Antarctica). *Mon. Wea. Rev.*, **118,** 779–793.

James, I. N., 1988: On the forcing of planetary-scale Rossby waves by Antarctica. *Quart. J. Roy. Meteor. Soc.*, **114,** 619–637.

——, 1989: The Antarctic drainage flow: Implications for hemispheric flow on the Southern Hemisphere. *Antarct. Sci.*, **1,** 279–290.

Jouzel, J., C. Lorius, J. R. Petit, C. Genthon, N. I. Barkov, V. M. Kotlyakov, and V. N. Petrov, 1987: Vostok ice core: A continuous isotope temperature record over the last climate cycle (160 000 years). *Nature*, **327,** 403–409.

Kitoh, A., K. Yamazaki, and T. Tokioka, 1990: The double-jet and semi-annual oscillations in the Southern Hemisphere simulated by the Meteorological Research Institute General Circulation Model. *J. Meteor. Soc. Japan*, **68**(2), 251–263.

Lorius, C., J. Jouzel, C. Ritz, L. Merlivart, N. I. Barkov, Y. S. Korotkevich, and V. M. Kotlyakov, 1985: A 150 000 year climate record from Antarctic ice. *Nature*, **316,** 591–596.

Manabe, S., 1969: Climate and ocean circulation. 1: The atmosphere circulation and the hydrology of the earth's surface. *Mon. Wea. Rev.*, **97,** 739–773.

——, J. Smagorinsky, and R. F. Strickler, 1965: Simulated climatology of a general circulation model with a hydrologic cycle. *Mon. Wea. Rev.*, **93,** 769–798.

Meehl, G. A., 1991: A reexamination of the mechanism of the semiannual oscillation in the Southern Hemisphere. *J. Climate*, **4,** 911–926.

——, and B. A. Albrecht, 1988: Tropospheric temperatures and the Southern Hemisphere circulation. *Mon. Wea. Rev.*, **116,** 953–960.

Murray, R. J., and I. Simmonds, 1991: A numerical scheme for tracking cyclone centers from digital data. Part II: Application to January and July general circulation model simulations. *Aust. Meteor. Mag.*, **39,** 167–180.

Oglesby, R. J., 1989: A GCM study of Antarctic glaciation. *Climate Dyn.*, **3,** 135–156.

Parish, T. R., 1984: A numerical study of strong katabatic winds over Antarctica. *Mon. Wea. Rev.*, **112,** 545–554.

——, and D. H. Bromwich, 1991: Continental-scale simulation of the Antarctic katabatic wind regime. *J. Climate*, **4,** 136–146.

Peixoto, J. P., and A. H. Oort, 1983: The atmospheric branch of the hydrological cycle and climate. *Variations in the Global Water Budget.* A. Street-Perrott, M. Beran, and R. Ratcliffe, Eds., D. Reidel, 5–65.

Prentice, M. L., and G. H. Denton, 1988: The deep-sea oxygen isotope record, the global ice sheet system and hominid evolution. *Evolutionary History of the "Robust" Australopithecines.* F. E. Grine, Ed., Aldine de Gruyter, 383–403.

Radok, U., 1973: On the energetics of surface winds over the Antarctic ice cap. Energy fluxes over polar surfaces. WMO Tech. Note 129, 69–100.

Ramanathan, V., E. J. Pitcher, R. C. Malone, and M. L. Blackmon, 1983: The response of a spectral general circulation model to refinements in radiative processes. *J. Atmos. Sci.*, **40,** 605–630.

Randel, W. J., and D. L. Williamson, 1990: A comparison of the climate simulated by the NCAR Community Climate Model (CCM1:R15) with ECMWF analyses. *J. Climate*, **3,** 608–633.

Rasch, P. J., and D. L. Williamson, 1990: Computational aspects of moisture transport in global models of the atmosphere. *Quart. J. Roy. Meteor. Soc.*, **116,** 1071–1090.

Schlesinger, M. E., 1984: Atmospheric general circulation model simulations of the modern Antarctic climate. *Environment of West Antarctica: Potential $CO_2$-Induced Changes,* National Academy Press, 155–196. [National Research Council, 2101 Constitution Avenue, N.W., Washington, D.C. 20418.]

Schwerdtfeger, W., 1970: The climate of the Antarctic. *World Survey of Climatology.* Vol. 14, S. Orvig, Ed., Elsevier, 253–355.

——, 1984: *Weather and Climate of the Antarctic.* Elsevier Science, 261 pp.

Shibata, K., and M. Chiba, 1990: Effects of radiation scheme on the surface temperature and wind over the Antarctic and on circumpolar lows. *Proc. NIPR Symp. Polar Meteor. Glaciol.*, **3,** 58–78. [National Institute of Polar Research, Itabashi-ku, Tokyo 173, Japan.]

Simmonds, I., 1990: Review: Improvements in general circulation model performance in simulating Antarctic climate. *Antarct. Sci.*, **2**(4), 287–300.

——, and W. F. Budd, 1991: Sensitivity of the southern hemispheric circulation to leads in the Antarctic pack ice. *Quart. J. Roy. Meteor. Soc.*, **117,** 1003–1024.

Stouffer, R. J., S. Manabe, and K. Bryan, 1989: Interhemispheric asymmetry in climate response to a gradual increase of atmospheric $CO_2$. *Nature*, **342,** 660–662.

Streten, N. A., 1963: Some observations of Antarctic katabatic winds. *Aust. Meteor. Mag.*, **42,** 1–23.

Taljaard, J. J., H. van Loon, H. L. Crutcher, and R. L. Jenne, 1969: *Climate of the Upper Air: Southern Hemisphere. Vol. 1. Temperature, Dew Points and Heights at Selected Pressure Levels.* NAVAIR-50-1C-55, 135 pp. [Commander, Naval Weather Service Command, Washington Naval Yard, Building 200, Washington, D.C. 20390.]

Tauber, G. M., 1960: Characteristics of Antarctic katabatic winds. *Antarctic Meteorology, Proc. Symp.*, Melbourne, The Australian Academy of Science, 52–64.

Tucker, G. B., 1991: Confidence in modeling future climate: A Southern Hemisphere perspective. *Clim. Change*, **18,** 195–204.

Turner, J., and M. Row, 1989: Mesoscale vortices in the British Antarctic Territory. *Polar and Arctic Lows,* P. F. Twitchell, E. A. Rasmussen, and K. L. Davidson, Eds., A. Deepak, 347–356.

van Loon, H., 1967: The half-yearly oscillations in middle and high southern latitudes and the coreless winter. *J. Atmos. Sci.*, **56,** 497–515.

——, J. J. Taljaard, T. Sasamori, J. London, D. V. Hoyt, K. Labitzke, and C. W. Newton, 1972: *Meteorology of the Southern Hemisphere, Meteor. Monogr.*, Vol. 13, C. W. Newton, Ed., Amer. Meteor. Soc., 263 pp.

Williamson, D. L., 1990: CCM progress report—July 1990. NCAR Tech. Note, NCAR/TN-351+PPR, 108 pp. [Available from the National Center for Atmospheric Research, Boulder, CO.]

——, J. T. Kiehl, V. Ramanathan, R. E. Dickinson, and J. J. Hack, 1987: Description of NCAR Community Climate Model (CCM1). NCAR Tech. Note, NCAR/TN-285-STR, 112 pp. [Available from the National Center for Atmospheric Research, Boulder, CO.]

Williamson, G. S., and D. L. Williamson, 1987: Circulation statistics from seasonal and perpetual January and July simulations with the NCAR Community Climate Model (CCM1):R15. NCAR Tech. Note, NCAR/TN-302-STR, 199 pp. [Available from the National Center for Atmospheric Research, Boulder, CO.]

Xu, J.-S., H. von Storch, and H. van Loon, 1990: The performance of four spectral GCMs in the Southern Hemisphere: The January and July climatology and the semiannual waves. *J. Climate*, **3,** 53–70.

Yamanouchi, T., and S. Kawaguchi, 1992: Cloud distribution in the Antarctic from AVHRR data and radiation measurements at the surface. *Int. J. Remote Sens.*, **13,** 111–127.